Inorganic Chemistry

Article

pubs.acs.org/IC

Tuning the Electronic and Steric Parameters of a Redox-Active Tris(amido) Ligand

Rui F. Munhá, Ryan A. Zarkesh, and Alan F. Heyduk*

Department of Chemistry, University of California, Irvine, California 92697-2025, United States

Supporting Information

ABSTRACT: A family of tantalum compounds was prepared to probe the electronic effects engendered by the addition of electron-donating or electron-withdrawing groups to the 4/4′ positions of the redox-active ligand derived from bis(2-isopropylamino-4-X-phenyl)amine [^{X,iPr}(NNN^{cat})H$_3$, X = F, H, Me, ^{t}Bu]). A general synthetic procedure for the ^{X,iPr}(NNN^{cat})H$_3$ ligand family was developed starting from the 4/4′ disubstituted diphenylamine derivative. A second ligand modification, incorporation of aromatic substituents at the flanking nitrogen moieties, was achieved via palladium-catalyzed cross-coupling to afford bis(2-3,5-dimethylphenylamino-4-methoxy-phenyl)amine ^{OMe,DMP}(NNN^{cat})H$_3$ (DMP = 3,5-C$_6$H$_3$Me$_2$), allowing a comparative study to the less sterically hindered isopropyl derivative. Treatment of the triamines with 1 equiv of TaMe$_3$Cl$_2$ generated the corresponding dichloro complexes ^{X,R}(NNN^{cat})TaCl$_2$(L) (L = empty or Et$_2$O) in high yields. These neutral dichloride derivatives reacted with [NBnEt$_3$][Cl] to produce the anionic trichloride derivatives [NBnEt$_3$][^{X,R}(NNN^{cat})TaCl$_3$], whereas the neutral dichloride derivatives reacted with chlorine atom donors to produce the neutral trichloride derivatives ^{X,R}(NNN^{sq})TaCl$_3$, containing the one-electron-oxidized form of the redox-active ligand. Aryl azides reacted with the ^{X,R}(NNN^{cat})TaCl$_2$(L) derivatives, resulting in nitrene transfer to tantalum and two-electron oxidation of the ligand platform to give ^{X,R}(NNN^{q})TaCl$_2$(=NR′) (R = iPr; X = OMe, F, H, Me; R′ = p-C$_6$H$_4$tBu, p-C$_6$H$_4$CF$_3$; and R = 3,5-C$_6$H$_3$Me$_2$; X = OMe; R′ = p-C$_6$H$_4$CH$_3$). Electrochemistry, UV−vis−NIR, IR, and EPR spectroscopies along with X-ray diffraction methods were used to characterize and compare complexes with different redox-active ligand derivatives in each oxidation state. This study demonstrates that while the ligand redox potentials can be adjusted over a 270 mV range through substitutions at the 4/4′ ring positions, the coordination chemistry and reactivity patterns at the bound tantalum center remain unchanged, suggesting that such ligand modifications can be used to tune the redox potentials of a complex for a particular substrate of interest.

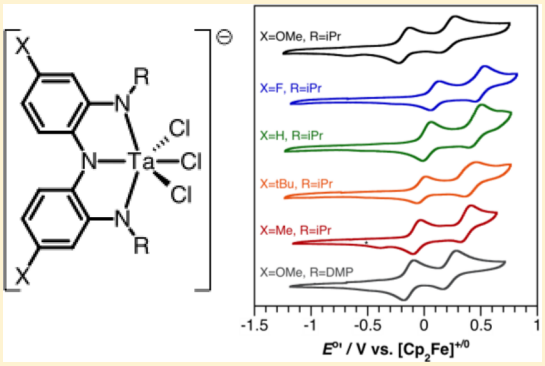

INTRODUCTION

Interest in noninnocent or redox-active ligands has increased owing to the recognition that these ligand platforms can be exploited to engender multielectron reactivity in coordination complexes.[1−14] Toward this end, one key feature of any redox-active ligand platform is the reduction potential(s) at which the ligand oxidation state changes in a coordination complex. While the coordinated metal ion modulates the ligand reduction potential(s), an appealing aspect of redox-active ligands is that these reduction potential(s) also may be tailored through systematic modifications to the ligand platform itself. Comparisons of ortho-quinone, ortho-iminoquinone, and ortho-diiminoquinone complexes of ruthenium(II) revealed reduction potentials in isostructural and isoelectronic complexes that varied by over 0.8 V.[15] More recently, Chirik and co-workers examined the addition of electron-donating and electron-withdrawing groups to the redox-active pyridinediimine (PDI) ligand.[16,17] In this Article, we report a detailed examination of the impact of electron-donating and electron-withdrawing groups on a topologically similar redox-active tris(amido) ligand platform.

Two related redox-active pincer ligands, (ONO) and ^{X,R}(NNN) of Chart 1, engender different multielectron reactivity when coordinated to tantalum. Both of these ligands are stable in three oxidation states when metal-bound: the trianionic catecholate forms, the dianionic semiquinonate forms, and the monoanionic quinonate forms.[1,6] These ligands afford isostructural and isoelectronic coordination complexes when bound to tantalum; however, the tantalum complexes display different reactivity due to redox potentials that vary by approximately 500 mV.[18] Whereas ^{OMe,iPr}(NNN^{cat})TaCl$_2$ reacted with phenyl azide to extrude N$_2$ and give the robust terminal imido complex ^{OMe,iPr}(NNN^{q})TaCl$_2$(=NPh),[19] the reaction of (ONO^{cat})TaCl$_2$ with phenyl azide resulted in nitrene coupling to afford azobenzene by a bimolecular four-electron reductive elimination.[20] Experimental evidence suggested that this latter reaction proceeds through an analogous terminal imido intermediate, but that the more strongly oxidizing (ONO^{q})$^-$ ligand drives the nitrene coupling

Received: June 13, 2013
Published: September 6, 2013

dx.doi.org/10.1021/ic401496w | Inorg. Chem. 2013, 52, 11244−11255

Chart 1

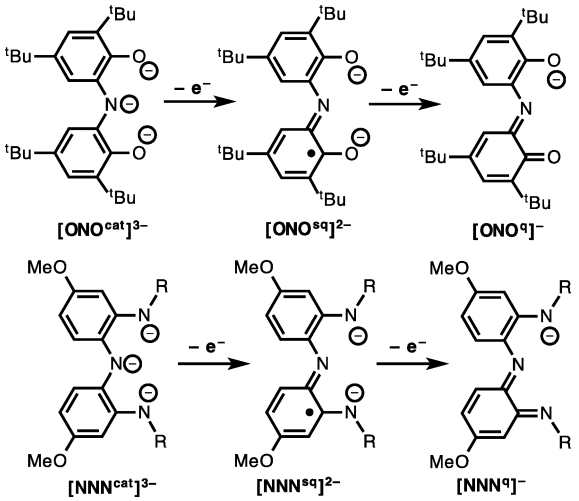

reaction.[6] While the stronger oxidizing nature of the $(ONO^{q})^{-}$ ligand compared to the $^{OMe,iPr}(NNN^{q})^{-}$ ligand is consistent with the prior results from Lever's studies on bidentate redox-active ligands,[15,21] we postulated that a secondary factor may be the inclusion of electron-donating methoxy groups into the (NNN) ligand backbone. As shown in Chart 2, these methoxy groups are in resonance with the redox-active π-system of the ligand and could further stabilize the quinonate form of the (NNN) ligand.

Chart 2

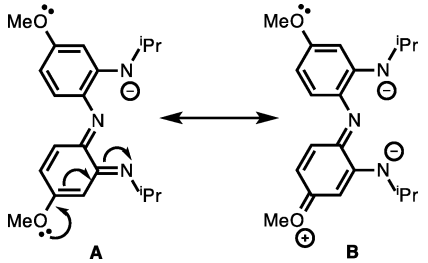

To assess the importance of ligand substituents on the electronic properties of the ^{X,R}(NNN) ligand platform, new ligand derivatives have been prepared containing different functional groups in the ligand backbone (X) and in the ligand arms (R). To determine the electronic influence of backbone substitution, five different $^{X,iPr}(NNN^{cat})H_3$ ligand derivatives were prepared (X = F, H, Me, tBu, and OMe), while the importance of the amido arm substituent was evaluated by comparing two derivatives, $^{OMe,R}(NNN^{cat})H_3$ (R = iPr; 3,5-$C_6H_3Me_2$). Isostructural tantalum complexes were prepared containing these redox-active ligands in all three ligand oxidation states of Chart 1. The metal complexes were characterized by NMR, EPR, UV–vis–NIR, and IR spectroscopies as appropriate, as well as by cyclic voltammetry and X-ray crystallography. Notably, changes to the ligand backbone functional groups (X) change the ligand-based redox potentials over a range of 270 mV, providing a logical approach for tuning the redox properties of a coordination complex during ligand synthesis. Conversely, changes to the amido substituent minimally affect the electronic properties of the coordination complex, yet afford afford different coordination isomers of the metal coordination sphere.

EXPERIMENTAL SECTION

General Considerations. The complexes described below are air and moisture sensitive, necessitating that manipulations be carried out under an inert atmosphere of argon or nitrogen gas using standard Schlenk, vacuum-line, and glovebox techniques. Ambient temperature in the glovebox was 27 °C. Hydrocarbon solvents were sparged with nitrogen and then deoxygenated and dried by passage through Q5 and activated alumina columns, respectively. Ethereal and halogenated solvents were sparged with nitrogen and then dried by passage through two activated alumina columns. Bis(4-methylphenyl)amine was purchased from TCI; isoamyl nitrite and *N*-chlorosuccinimide were purchased from Alfa Aesar and used without further purification. The compounds bis(4-tert-butylphenyl)amine,[22] bis(4-fluorophenyl)-amine,[23] $^{H,iPr}(NNN^{cat})H_3$ (**2c**),[24] $TaMe_3Cl_2$,[25] and $^{OMe,iPr}(NNN^{cat})$-$TaCl_2$ (**3a**)[19] were prepared according to previously reported synthetic methodologies. tert-Butylisocyanide was purchased from Aldrich, dried with CaH_2, and distilled prior to use. $[^{n}Bu_4N][PF_6]$ and $[NBnEt_3][Cl]$ were recrystallized three times from hot methanol and dried under high vacuum.

Spectroscopic Methods. NMR spectra were collected on a Bruker Avance 600, 500, or 400 MHz spectrometer in dry, degassed deuterated solvents. ^{1}H NMR spectra were referenced to TMS using the residual proteo impurities of the solvent; ^{13}C NMR spectra were referenced to TMS using the natural-abundance ^{13}C impurities of the solvent. All chemical shifts are reported using the standard δ notation in parts per million; positive chemical shifts are to a higher frequency of the given reference. Infrared spectra were recorded as KBr pellets with a Perkin-Elmer Spectrum One FTIR spectrophotometer. Electronic absorption spectra were recorded with a Perkin-Elmer Lambda 800 UV–vis spectrophotometer or a Perkin-Elmer Lambda 900 UV–vis spectrophotometer equipped with a NIR detector, both using 1 cm quartz cuvettes. APCI-MS data was collected on a Waters LCT Premier mass spectrometer. EPR spectra were collected on a Bruker EMX X-band spectrometer equipped with an ER041XG microwave bridge. Spectra for EPR samples were collected using the following spectrometer settings: attenuation = 20 dB, microwave power = 2.017 mW, frequency = 9.79 GHz; sweep width = 300 G, modulation amplitude = 9.02 G, gain = 2.00×10^{3}, conversion time = 10.24 ms, time constant = 81.92 ms, and resolution = 2048 points. The EPR spectra were modeled using MATLAB, assuming an isotropic signal and hyperfine coupling to three equivalent nitrogen atoms. Elemental analyses were collected on a Perkin-Elmer 2400 Series II CHNS/O analyzer.

Electrochemical Methods. Electrochemical experiments were performed on a Gamry Series G 300 potentiostat/galvanostat/ZRA (Gamry Instruments, Warminster, PA) using a 1.5 mm diameter platinum disk working electrode, a platinum wire auxiliary electrode, and a silver wire reference electrode. Electrochemical experiments were performed at ambient temperature (27 °C) under a dinitrogen atomosphere in a MeCN solution containing 0.1 M $[^{n}Bu_4N][PF_6]$ as the supporting electrolyte and 1 mM of the desired analyte. All potentials were referenced to $[Cp_2Fe]^{+/0}$, using $[Cp_2Co][PF_6]$ as an internal standard (−1.336 V vs $[Cp_2Fe]^{+/0}$). Under our conditions the typical solvent window is from a reductive limit of −2.00 V to an oxidative limit of +2.00 V.

X-ray Diffraction Methods. X-ray diffraction data for **3b**–**3f**, **6f**, **7a**, and **7d** were collected on crystals mounted on glass fibers with Paratone oil using a Bruker CCD platform diffractometer equipped with a CCD detector. Measurements were carried out at 88 K using Mo Kα (λ = 0.710 73 Å) radiation, which was wavelength selected with a single-crystal graphite monochromator. The SMART[26] program package was used to determine the unit-cell parameters and for data collection. A full sphere of data was collected for each crystal structure. The raw frame data were processed using SAINT[27] and SADABS[28] to yield the reflection data files. Subsequent calculations were carried out using the SHELXTL[29] program suite. Structures were solved by direct

dx.doi.org/10.1021/ic401496w | *Inorg. Chem.* 2013, 52, 11244–11255

methods and refined on F^2 by full-matrix least-squares techniques to convergence. Analytical scattering factors[30] for neutral atoms were used throughout the analyses. Hydrogen atoms were generated at calculated positions and their positions refined using the standard riding models. ORTEP[31] diagrams were generated using ORTEP-3 for Windows, and all thermal ellipsoids are drawn at the 50% probability level. Diffraction collection and refinement data are available in the Supporting Information.

General Preparation of Bis(4-X-2-nitrophenyl)amine. This preparation was adapted from a previous report.[19] Here is outlined a typical example. A round-bottom flask equipped with a stir bar was charged with a solution of bis(4-fluorophenyl)amine (5.00 g, 24 mmol, 1 equiv) in 10 mL of concentrated nitric acid and 45 mL of glacial acetic acid. The solution was stirred for 10 min in an ice−water bath before isoamyl nitrite (8.75 g, 75 mmol, 3 equiv) was slowly dripped into solution over the course of 2 min. After stirring for additional 5 min, an orange precipitate was collected and washed with diethyl ether.

Bis(4-fluoro-2-nitrophenyl)amine. This material was prepared in 71% yield (5.04 g). ^{1}H NMR (400 MHz, $CDCl_3$) δ/ppm: 10.68 (s, 1H, N−H), 7.91 (dd, J = 2.8 Hz, 2H, aryl-H), 7.47 (m, 2H, aryl-H), 7.32 (m, 2H, aryl-H). ^{13}C{^{1}H} NMR (77 Hz, $CDCl_3$) δ/ppm: 133.8 (aryl-C), 123.1 (d, J = 92 Hz, aryl-C), 122.9 (aryl-C), 121.3 (d, J = 30 Hz, aryl-C), 113.3 (d, J = 100 Hz, aryl-C), 113.1 (aryl-C). ^{19}F{^{1}H} NMR δ/ppm: −117.9. MS (ESI$^+$) m/z: 295.3 (M^+), 296.1 (MH^+).

Bis(4-tert-butyl-2-nitrophenyl)amine. After stirring for 10 min, the solution was treated with 50 mL of water, and the acidic solution was neutralized with $NaHCO_3$ to pH 7. The organic layer was extracted with dichloromethane (3 × 60 mL). The extracts were collected and dried under vacuum. The resulting red-orange residue was chromatographed on silica gel with a 10:1 hexanes/ethyl acetate (v/v %) elutent, and the red solution was collected and dried to give bis(4-tert-butyl-2-nitrophenyl)amine (2.66 g, 40%). ^{1}H NMR (500 MHz, $CDCl_3$) δ/ppm: 10.85 (s, 1H, N−H), 7.91 (d, J = 2 Hz, 2H, aryl-H), 7.53 (dd, J = 2 Hz, 2H, aryl-H), 7.51 (s, 2H, aryl-H), 1.35 (s, 18H, ^{t}Bu). ^{13}C{^{1}H} NMR (77 Hz, $CDCl_3$) δ/ppm: 145.3 (aryl-C), 138.0 (aryl-C), 135.1 (aryl-C), 132.3 (aryl-C), 122.9 (aryl-C), 119.7 (aryl-C), 34.5 ($C(CH_3)_3$), 31.0 ($C(CCH_3)_3$. MS (ESI$^+$) m/z: 371.3 (M^+), 372.2 (MH^+).

General Preparation of Bis(2-amino-4-X-phenyl)amine. The new compounds were all prepared by a common procedure which is outlined for a typical example. A 250 mL Schlenk flask equipped with a stir bar was filled with solid bis(4-methyl-2nitro-phenyl)amine (1.24 g, 4.3 mmol, 1 equiv), Zn powder (100 mesh, 3.712 g, 56.8 mmol, 14 equiv), and NH_4Cl (2.78 g, 52 mmol, 13 equiv) before the contents were exposed to vacuum. Backfilling the Schlenk flask with inert gas, 60 mL of THF was cannula transferred into the flask before a reflux condenser was attached to the Schlenk flask. The solution stirred at gentle reflux for 16 h before the pale yellow solution was cooled and filtered under N_2. The yellow solution was dried under vacuum to a yellow-brown oil.

*Bis(2-amino-4-fluorophenyl)amine (**1b**).* A slight modification of the procedure was used: Zn powder (14.04 g, 215 mmol, 30 equiv) and NH_4Cl (8.78 g, 164 mmol, 20 equiv). Yield 98% (1.65 g). ^{1}H NMR (400 MHz, C_6D_6) δ/ppm: 6.31 (td, J_{HF} = 11 Hz, J_{HH} = 3.5 Hz, 2H, aryl-H), 6.27 (d, J_{HH} = 5.5 Hz, 2H, aryl-H), 6.12 (dd, $^4J_{HH}$ = 3.5 Hz, $^3J_{HH}$ = 9 Hz, 2H, aryl-H), 2.99 (br, 5H, N−H). ^{13}C{^{1}H} NMR (77 Hz, $CDCl_3$) δ/ppm: 161.4 (aryl-C), 140.7 (aryl-C), 123.2 (aryl-C), 121.8 (d, J = 48 Hz, aryl-C), 104.9 (d, J = 111 Hz, aryl-C), 102.6 (d, J = 129 Hz, aryl-C), 113.1 (aryl-C). ^{19}F{^{1}H} NMR δ/ppm: −120.3. MS (ESI$^+$) m/z: 235.1 (M^+), 236.1 (MH^+).

*Bis(2-amino-4-methylphenyl)amine (**1d**).* This material was prepared in 90% yield (1.27 g). ^{1}H NMR (500 MHz, C_6D_6) δ/ppm: 6.62 (d, J = 8 Hz, 2H, aryl-H), 6.51 (d, J = 8 Hz, 2H, aryl-H), 6.26 (s, 2H, aryl-H), 3.08 (br, 5H, N−H), 2.15 (s, 6H, aryl-CH_3). ^{13}C{^{1}H} NMR (128 Hz, C_6D_6) δ/ppm: 138.8 (aryl-C), 132.5 (aryl-C), 129.4 (aryl-C), 120.7 (aryl-C), 120.3 (aryl-C), 117.3 (aryl-C), 21.1 (aryl-CH_3). MS (ESI$^+$) m/z: 227.3 (M^+), 228.2 (MH^+).

*Bis(2-amino-4-tert-butylphenyl)amine (**1e**).* This material was prepared in 95% yield (1.50 g). ^{1}H NMR (500 MHz, C_6D_6) δ/ppm: 6.69 (m, 4H, aryl-H), 6.59 (d, J = 1.5 Hz, 2H, aryl-H), 3.08 (br, 5H, N−H), 1.28 (s, 18H, aryl-tBu). ^{13}C{^{1}H} NMR (128 Hz, C_6D_6) δ/ppm: 145.9 (aryl-C), 138.5 (aryl-C), 129.4 (aryl-C), 120.3 (aryl-C), 116.5 (aryl-C), 113.6 (aryl-C), 34.3 (aryl-$C(CH_3)_3$), 31.7 (aryl-$C(CH_3)_3$). MS (ESI$^+$) m/z: 311.2 (M^+), 312.2 (MH^+).

General Preparation of Bis(2-isopropylamino-4-X-phenyl)-amine (^{X,iPr}(NNN^{cat})H$_3$). The new ligand precursors were all prepared by a common procedure which is outlined for a typical example. A Schlenk flask was charged with bis(2-amino-4-methyl-phenyl)amine (0.969 g, 4.8 mmol, 1 equiv) and a stir bar. Under an inert atmosphere, 60 mL of degassed MeOH was cannula transferred to the flask. Degassed acetone (0.78 mL, 10.6 mmol, 2.2 equiv) and degassed concentrated HCl (0.87 mL, 10.5 mmol, 2.2 equiv) were transferred via microsyringe to the reaction flask resulting in the reaction mixture turning green. The green solution stirred in an ice−water bath for 20 min before a solid addition tube filled with $NaCNBH_3$ (1.223 g, 19.5 mmol, 4 equiv) was attached to the Schlenk flask. The solid addition tube was slowly upended as the green solution stirred. After stirring for 12 h the yellow solution was dried under vacuum, and the yellow-red residue was treated with water. The organic layer was extracted with CH_2Cl_2 (3 × 20 mL). The combined organic layers were dried over $MgSO_4$, and the solvent was removed under vacuum to a yellow-brown oil.

*Bis(2-isopropylamino-4-fluorophenyl)amine, ^{F,iPr}(NNN^{cat})H$_3$ (**2b**).* This material was prepared in 71% yield (0.56 g). ^{1}H NMR (600 MHz, C_6D_6) δ/ppm: 6.35 (overlapping, 6H, aryl-H), 3.77 (s, 1H, N−H), 3.62 (s, 2H, N−H), 3.09 (sept, $^3J_{HH}$ = 7.8 Hz, 2H, $CH(CH_3)_2$), 0.80 (d, $^3J_{HH}$ = 7.8 Hz, 12H, $CH(CH_3)_3$) . ^{13}C{^{1}H} NMR (128 Hz, C_6D_6) δ/ppm: 146.3 (aryl-C), 136.8 (aryl-C), 130.9 (aryl-C), 120.8 (aryl-C), 115.5 (aryl-C), 109.9 (aryl-C), 34.5 (aryl-$C(CH_3)_3$), 31.7 (aryl-$C(CH_3)_3$), 31.7 ($CH(CH_3)_2$). ^{19}F{^{1}H} NMR δ/ppm: −118.0. MS (ESI$^+$) m/z: 319.2 (M^+), 320.2 (MH^+).

*Bis(2-isopropylamino-4-methyl-phenyl)amine, ^{Me,iPr}(NNN^{cat})H$_3$ (**2d**).* This material was prepared in 71% yield (1.06 g). ^{1}H NMR (500 MHz, C_6D_6) δ/ppm: 6.73 (d, $^3J_{HH}$ = 8 Hz, 2H, aryl-H), 6.63 (s, 2H, aryl-H), 6.53 (d, $^3J_{HH}$ = 8 Hz, 2H, aryl-H), 4.86 (br, 3H, N−H), 3.43 (sept, $^3J_{HH}$ = 6 Hz, 2H, $CH(CH_3)_2$), 2.22 (s, 6H, aryl-CH_3), 0.98 (d, $^3J_{HH}$ = 6.5 Hz, 12H, $CH(CH_3)_3$). ^{13}C{^{1}H} NMR (128 Hz, C_6D_6) δ/ppm: 133.0 (aryl-C), 130.2 (aryl-C), 123.1 (aryl-C), 121.4 (aryl-C), 119.7 (aryl-C), 114.8 (aryl-C), 45.2 ($CH(CH_3)_2$), 22.6 (aryl-CH_3), 21.5 ($CH(CH_3)_3$). MS (ESI$^+$) m/z: 311.2 (M^+), 312.2 (MH^+).

*Bis(2-isopropylamino-4-tert-butylphenyl)amine, ^{tBu,iPr}(NNN^{cat})H$_3$ (**2e**).* This material was prepared in 96% yield (0.36 g). ^{1}H NMR (500 MHz, C_6D_6) δ/ppm: 6.99 (s, 2H, aryl-H), 6.63 (d, $^3J_{HH}$ = 10 Hz, 2H, aryl-H), 6.53 (dd, $^3J_{HH}$ = 7.5 Hz, $^4J_{HH}$ = 2.5 Hz, 2H, aryl-H), 5.28 (br, 2H, N−H), 4.70 (br, 1H, N−H), 3.52 (sept, $^3J_{HH}$ = 8 Hz, 2H, $CH(CH_3)_2$), 1.32 (s, 18H, aryl-^{t}Bu), 1.02 (d, $^3J_{HH}$ = 8 Hz, 12H, $CH(CH_3)_3$) . ^{13}C{^{1}H} NMR (128 Hz, C_6D_6) δ/ppm: 146.3 (aryl-C), 136.8 (aryl-C), 130.9 (aryl-C), 120.8 (aryl-C), 115.5 (aryl-C), 109.9 (aryl-C), 34.5 (aryl-$C(CH_3)_3$), 31.7 (aryl-$C(CH_3)_3$), 31.7 (CH-$(CH_3)_2$). MS (ESI$^+$) m/z: 395.4 (M^+), 396.5 (MH^+).

*Bis(2-3,5-dimethylphneyl-amino-4-methoxyphenyl)amine, ^{OMe,DMP}(NNN^{cat})H$_3$ (**2f**).* A Schlenk flask was charged with $Pd_2(dba)_3$ (0.120 g, 0.13 mmol, 0.06 equiv), racemic-BINAP (0.240 g, 0.39 mmol, 0.18 equiv,) and 5 mL of THF. The solution was stirred for 2 h at room temperature and transferred to a Schlenk flask containing ^{OMe}(NNN^{cat})H$_5$ (0.60 g, 2.31 mmol, 1.2 equiv), 3,5-methyl-bromobenzene (0.76 g, 4.10 mmol, 2 equiv), and NaO^{t}Bu (0.55 g, 5.74 mmol, 2.8 equiv). The mixture was refluxed for 48 h, taken to dryness, and the resulting slurry was extracted with diethyl ether. The mixture was filtered and the solution taken to dryness. The ^{1}H NMR spectrum indicated the formation of ^{OMe,DMP}(NNN^{cat})H$_3$ with 95% purity. Pentane wash of the solids gave 0.59 g of the parent compound in 62% yield. ^{1}H NMR (400 MHz; C_6D_6; 298 K) δ/ppm: 7.06 (d, $^4J_{HH}$ = 2.8 Hz, 2H, aryl-H), 6.94 (d, $^3J_{HH}$ = 8.7 Hz, 2H, aryl-H), 6.54 (s, 4H, aryl-H), 6.50 (dd, $^3J_{HH}$ = 8.7 Hz, $^4J_{HH}$ = 2.8 Hz, 2H, aryl-H), 6.48 (s, 2H, aryl-H), 5.49 (s, 2H, N−H), 5.09 (s, 1H, N−H), 3.34 (s, 6H, O−CH_3), 2.08 (s, 12H, aryl-CH_3). ^{13}C{^{1}H} NMR (128 MHz; C_6D_6; 298 K) δ/ppm: 156.4 (ipso-C), 144.1 (ipso-C), 138.9 (ipso-C), 136.5 (ipso-C), 130.2 (ipso-C), 123.1 (aryl-C), 121.5 (aryl-C), 116.0 (aryl-

C), 108.1 (aryl-C), 106.6 (aryl-C), 55.1 (OCH_3), 21.4 (aryl-CH_3). MS (ESI^+) m/z: 466.1 (M^+).

General Preparation of $^{X,R}(NNN^{cat})TaCl_2$. The new compounds were all prepared by a common procedure which is outlined for a typical example. A 50 mL round-bottom flask equipped with a stir bar was charged with $TaMe_3Cl_2$ (0.471 g, 1.59 mmol, 1 equiv) dissolved in 30 mL of diethyl ether and frozen in a cold well. A 0.3 M solution of $^{Me,iPr}(NNN^{cat})H_3$ in toluene (5.28 mL, 1.59 mmol, 1 equiv) was diluted with 10 mL of diethyl ether and chilled to −35 °C. The yellow $TaMe_3Cl_2$ solution was removed from the liquid nitrogen filled cold well, and just as the solution thawed the ligand solution was slowly added to the flask with vigorous stirring. The reaction was allowed to warm to room temperature and continued to stir overnight. The dark red solution was concentrated down 5 mL before the solution was diluted with 15 mL of pentane to give a brick red precipitate. The solid was isolated by filtration and dried under vacuum. X-ray quality crystals of **3b**, **3c**, **3d**, **3e**, **3f**·Et_2O were obtained from chilled (−35 °C), saturated diethyl ether/pentane solutions.

*$^{F,iPr}(NNN^{cat})TaCl_2$ (**3b**).* This material was prepared in 87% yield (0.32 g). Anal. Calcd for $C_{18}H_{20}N_3F_2Cl_2Ta$: C, 38.05; H, 3.55; N, 7.40. Found: C, 37.80; H, 3.50; N, 7.30. ^1H NMR (500 MHz, C_6D_6) δ/ppm: 7.02 (td, J_{HF} = 5.5 Hz, J_{HH} = 2.5 Hz, 2H, aryl-H), 6.39 (overlapping, 4H, aryl-H), 4.40 (sept, $^3J_{HH}$ = 6.5 Hz, 2H, $CH(CH_3)_2$), 1.18 (d, ^3J = 5 Hz, 12H, $CH(CH_3)_2$). $^{13}C\{^1H\}$ NMR (128 Hz, C_6D_6) δ/ppm: 160.1 (ipso-C), 146.6 (aryl-C), 143.8 (aryl-C), 114.1 (d, J_{CF} = 24 Hz, aryl-C), 106.5 (aryl-C), 107.3 (d, J_{CF} = 24 Hz, aryl-C), 99.9 (d, J_{CF} = 24 Hz, aryl-C), 48.1 ($CH(CH_3)_2$), 17.0 ($CH(CH_3)_3$). ^{19}F $\{^1H\}$ NMR δ/ppm: −122.6. UV−vis (toluene) λ_{max}/nm (ε/M^{-1} cm^{-1}): 308 (17 300).

*$^{H,iPr}(NNN^{cat})TaCl_2$ (**3c**).* This material was prepared in 87% yield (0.65 g). Anal. Calcd for $C_{18}H_{22}N_3Cl_2Ta$: C, 40.62; H, 4.17; N, 7.89. Found: C, 40.87; H, 4.20; N, 8.05. ^1H NMR (500 MHz, C_6D_6) δ/ppm: 7.52 (br, 2H, aryl-H), 6.70 (br, 4H, aryl-H), 6.52 (br, 2H, aryl-H), 4.62 (br, 2H, $CH(CH_3)_2$), 1.35 (s, 12H, $CH(CH_3)_2$). $^{13}C\{^1H\}$ NMR (128 Hz, C_6D_6) δ/ppm: 129.1 (ipso-C), 128.9 (ipso-C), 128.6 (aryl-C), 121.9 (aryl-C), 115.3 (aryl-C), 111.9 (aryl-C), 48.1 ($CH(CH_3)_2$), 17.4 ($CH(CH_3)_3$). UV−vis (toluene) λ_{max}/nm (ε/M^{-1} cm^{-1}): 293 (29 100).

*$^{Me,iPr}(NNN^{cat})TaCl_2$ (**3d**).* This material was prepared in 72% yield (0.17 g). Anal. Calcd for $C_{20}H_{26}N_3Cl_2Ta$: C, 42.87; H, 4.68; N, 7.50. Found: C, 42.50; H, 4.60; N, 7.50. ^1H NMR (600 MHz, C_6D_6) δ/ppm: 7.47 (d, $^3J_{HH}$ = 7.8 Hz, 2H, aryl-H), 6.53 (d, $^3J_{HH}$ = 6.5 Hz, 2H, aryl-H), 6.48 (s, 2H, aryl-H), 4.62 (sept, $^3J_{HH}$ = 7.8 Hz, 2H, $CH(CH_3)_2$), 2.25 (s, 6H, aryl-CH_3), 1.40 (d, $^3J_{HH}$ = 6.5 Hz, 12H, $CH(CH_3)_3$). $^{13}C\{^1H\}$ NMR (128 Hz, C_6D_6) δ/ppm: 146.1 (ipso-C), 130.7 (ipso-C), 129.0 (ipso-C), 122.1 (aryl-C), 114.4 (aryl-C), 112.1 (aryl-C), 47.6 ($CH(CH_3)_2$), 20.7 (aryl-CH_3), 17.1 ($CH(CH_3)_3$). UV−vis (toluene) λ_{max}/nm (ε/M^{-1} cm^{-1}): 300 (19 500).

*$^{tBu,iPr}(NNN^{cat})TaCl_2$ (**3e**).* This material was prepared in 72% yield (0.35 g). Anal. Calcd for $C_{26}H_{38}N_3Cl_2Ta$: C, 48.46; H, 5.94; N, 6.52. Found: C, 48.10; H, 5.80; N, 6.45. ^1H NMR (500 MHz, C_6D_6) δ/ppm: 7.55 (d, $^3J_{HH}$ = 8 Hz, 2H, aryl-H), 6.79 (overlapping, 4H, aryl-H), 4.67 (sept, $^3J_{HH}$ = 6 Hz, 2H, $CH(CH_3)_2$), 1.45 (d, $^3J_{HH}$ = 5.5 Hz, 12H, $CH(CH_3)_3$), 1.31 (s, 18H, aryl-$C(CH_3)_3$). $^{13}C\{^1H\}$ NMR (128 Hz, C_6D_6) δ/ppm: 146.3 (ipso-C), 145.8 (ipso-C), 144.4 (ipso-C), 118.7 (aryl-C), 114.4 (aryl-C), 109.1 (aryl-C), 47.9 ($CH(CH_3)_2$), 34.2 ($C(CH_3)_3$), 31.8 ($C(CH_3)_3$), 17.4 ($CH(CH_3)_3$). UV−vis (toluene) λ_{max}/nm (ε/M^{-1} cm^{-1}): 335 (18 300).

*$^{OMe,DMP}(NNN^{cat})TaCl_2(OEt_2)$ (**3f**·Et_2O).* This material was prepared in 76% yield (0.47 g). Anal. Calcd for $C_{34}H_{40}N_3O_3Cl_2Ta$: C, 51.66; H, 5.10; N, 5.32. Found: C, 52.05; H, 4.99; N, 5.19. ^1H NMR (500 MHz, C_6D_6) δ/ppm: 7.36 (br, 2H, aryl-H), 7.12 (s, 4H, aryl-H), 6.60 (m, 2H, aryl-H), 6.37 (br, 2H, Ph-H), 5.95 (br, 2H, Ph-H), 3.45 (m, 4H, OCH_2CH_3), 3.29 (br, 6H, OCH_3), 2.00 (s, 12H, Ph−CH_3), 1.04 (m, 4H, OCH_2CH_3). $^{13}C\{^1H\}$ NMR (128 Hz, C_6D_6) δ/ppm: 157.1 (ipso-OCH_3), 152.6 (ipso-C), 142.3 (ipso-C), 139.5 (ipso-C), 129.8 (ipso-C), 126.5 (aryl-C), 119.4 (aryl-C), 114.4 (aryl-C), 107.6 (aryl-C), 99.5 (aryl-C), 66.7 (OCH_2CH_3), 55.0 (aryl-OCH_3), 20.8 (aryl-CH_3), 14.4 (OCH_2CH_3). UV−vis (toluene) λ_{max}/nm (ε/M^{-1} cm^{-1}): 309 (29 200), 1050 (500).

General Preparation of $^{X,R}(NNN^{cat})TaCl_2(CN^tBu)$. The new compounds were all prepared by a common procedure which is outlined for a typical example. A 20 mL scintillation vial equipped with a stir bar was filled with solid $^{tBu,iPr}(NNN^{cat})TaCl_2$ (0.05 g, 0.08 mmol, 1 equiv) and dissolved with 5 mL of toluene. As the red solution stirred, tert-butylisocyanide (0.01 g, 0.12 mmol, 1.5 equiv) was slowly added to the solution via microsyringe causing an immediate color change to dark red. After stirring for 3 h the volatiles were removed under reduced pressure leaving the product as a dark red solid that was washed with pentane.

*$^{F,iPr}(NNN^{cat})TaCl_2(CN^tBu)$ (**4b**).* This material was prepared in 89% yield (0.11 g). Anal. Calcd for $C_{18}H_{20}N_3F_2Cl_2Ta$: C, 42.41; H, 4.49; N, 8.60. Found: C, 41.63; H, 4.50; N, 7.47. ^1H NMR (400 MHz; C_6D_6) δ/ppm: 6.92 (m, 2H, aryl-H), 6.38−6.27 (overlapping, 4H total, aryl-H), 5.43 (m, 2H, $CH(CH_3)_2$), 1.28 (br, 12H, $CH(CH_3)_2$), 0.54 (s, 9H, ($CN(C(CH_3)_3$). $^{13}C\{^1H\}$ NMR (128 MHz; C_6D_6, 298 K) δ/ppm: 149.5 ($CN(C(CH_3)_3$), 140.8 (ipso-C), 114.7 (d, J_{CF} = 24 Hz, aryl-C), 106.9 (d, J_{CF} = 23 Hz, aryl-C), 100.2 (d, J_{CF} = 10 Hz, aryl-C), 50.2 ($CH(CH_3)_2$), 28.9 ($CN(C(CH_3)_3$), 20.3 ($CN(C(CH_3)_3$), 16.5 ($CH(CH_3)_2$). ^{19}F $\{^1H\}$ NMR δ/ppm: −121.9. IR (KBr) $\nu_{CN(CNtBu)}$/cm^{-1}: 2203.

*$^{H,iPr}(NNN^{cat})TaCl_2(CN^tBu)$ (**4c**).* This material was prepared in 85% yield (0.05 g). Anal. Calcd for $C_{18}H_{22}N_3Cl_2Ta$: C, 44.89; H, 5.08; N, 9.10. Found: C, 45.13; H, 5.54; N, 8.69. ^1H NMR (400 MHz; C_6D_6) δ/ppm: 7.39 (d, $^3J_{HH}$ = 8, 2H, aryl-H), 6.62 (td, $^3J_{HH}$ = 8 Hz, $^4J_{HH}$ = 1 Hz, 2H, aryl-H), 6.56 (t, $^3J_{HH}$ = 8 Hz, 2H, aryl-H), 6.46 (d, $^3J_{HH}$ = 8 Hz, 2H, aryl-H), 5.63 (m, 2H, $CH(CH_3)_2$), 1.44 (d, $^3J_{HH}$ = 7 Hz, 12H, $CH(CH_3)_2$), 0.52 (s, 9H, ($CN(C(CH_3)_3$). ^{13}C NMR $\{^1H\}$ (128 MHz; C_6D_6) δ/ppm: 148.9 (ipso-C), 144.9 (CN), 128.3 (ipso-C), 122.5 (aryl-C), 121.3 (aryl-C), 116.0 (aryl-C), 112.6 (aryl-C), 49.9 ($CH(CH_3)_2$), 28.9 ($CN(C(CH_3)_3$), 20.9 ($CN(C(CH_3)_3$), 16.9 ($CH(CH_3)_2$). UV−vis (toluene) λ_{max}/nm (ε/M^{-1} cm^{-1}): 310 (11 000). IR (KBr) $\nu_{CN(CNtBu)}$/cm^{-1}: 2203.

*$^{Me,iPr}(NNN^{cat})TaCl_2(CN^tBu)$ (**4d**).* Yield is quantitative (0.04 g). Anal. Calcd for $C_{25}H_{35}N_4Cl_2Ta$: C, 46.67; H, 5.48; N, 8.71. Found: C, 46.63; H, 5.70; N, 8.88. ^1H NMR (600 MHz; C_6D_6) δ/ppm: 7.33 (d, $^3J_{HH}$ = 8 Hz, 2H, aryl-H), 6.45 (d, $^3J_{HH}$ = 8 Hz, 2H, aryl-H), 6.43 (s, 2H, aryl-H), 5.64 (m, 2H, $CH(CH_3)_2$), 2.23 (s, 6H, aryl-CH_3), 1.49 (d, $^3J_{HH}$ = 6 Hz, 12H, $CH(CH_3)_2$), 0.57 (s, 9H, ($CN(C(CH_3)_3$). $^{13}C\{^1H\}$ NMR (128 MHz; C_6D_6) δ/ppm: 149.1 (ipso-C), 142.9 (CN), 131.7 (ipso-C), 128.6 (aryl-C), 122.1 (aryl-C), 115.6 (aryl-C), 113.2 (aryl-C), 49.8 ($CH(CH_3)_2$), 29.0 ($CN(C(CH_3)_3$), 20.9 (overlapping, aryl-CH_3 and $CN(C(CH_3)_3$), 17.0 ($CH(CH_3)_2$). IR (KBr) $\nu_{CN(CNtBu)}$/cm^{-1}: 2198.

*$^{tBu,iPr}(NNN^{cat})TaCl_2(CN^tBu)$ (**4e**).* Yield is quantitative (0.06 g). Anal. Calcd for $C_{31}H_{47}N_4Cl_2Ta$: C, 51.17; H, 6.51; N, 7.70. Found: C, 51.71; H, 6.69; N, 7.70. ^1H NMR (400 MHz; C_6D_6) δ/ppm: 7.40 (d, $^3J_{HH}$ = 9 Hz, 2H, aryl-H), 6.73−6.66 (overlapping, 4H, aryl-H), 5.65 (m, 2H, $CH(CH_3)_2$), 1.52 (d, $^3J_{HH}$ = 6 Hz, 12H, $CH(CH_3)_2$), 1.24 (s, 18H, $C(CH_3)_3$), 0.51 (s, 9H, ($CN(C(CH_3)_3$). $^{13}C\{^1H\}$ NMR (128 MHz; C_6D_6) δ/ppm: 148.9 (ipso-C), 145.1(CN), 142.9 (ipso-C), 118.3 (aryl-C), 115.2 (aryl-C), 109.9 (aryl-C), 49.8 ($CH(CH_3)_2$), 34.0 ($C(CH_3)_3$), 31.9 ($C(CH_3)_3$), 28.9 ($CN(C(CH_3)_3$), 21.2 ($CN(C-(CH_3)_3$), 17.2 ($CH(CH_3)_2$). IR (KBr) $\nu_{CN(CNtBu)}$/cm^{-1}: 2203.

*$^{OMe,DMP}(NNN^{cat})TaCl_2(CN^tBu)$ (**4f**).* Yield is quantitative (0.06 g). Anal. Calcd for $C_{35}H_{39}N_4O_2Cl_2Ta$: C, 52.58; H, 4.92; N, 7.01. Found: C, 53.08; H, 4.95; N, 6.61. ^1H NMR (500 MHz; C_6D_6) δ/ppm: 7.53 (s, 2H, Ph-H), 7.23 (d, $^3J_{HH}$ = 9 Hz, 2H, Ph-H), 6.89 (s, 2H, Ph-H), 6.63 (s, 2H, Ph-H), 6.29 (d, $^3J_{HH}$ = 9 Hz, 2H, Ph-H), 5.87 (m, 2H, Ph-H), 3.23 (s, 6H, O−CH_3), 2.11 (s, 6H, Ph−CH_3), 2.00 (s, 6H, Ph−CH_3), 0.80 (s, 9H, $C(CH_3)_3$). $^{13}C\{^1H\}$ NMR (118 Hz, C_6D_6) δ/ppm: 158.1 (ipso-C), 154.6 (ipso-C), 144.4 (CN), 140.2 (ipso-C), 138.7 (ipso-C), 135.1 (ipso-C), 129.9 (aryl-C), 126.8 (aryl-C), 125.3 (aryl-C), 115.6 (aryl-C), 108.3 (aryl-C), 99.0 (aryl-C), 55.1 (aryl-OCH_3), 29.1 ($CN(C(CH_3)_3$), 21.3 (aryl-CH_3). IR (KBr) $\nu_{CN(CNtBu)}$/cm^{-1}: 2212.

General Preparation of $[NEt_3Bn][^{X,R}(NNN^{cat})TaCl_3]$. The new compounds were all prepared by a common procedure which is outlined for a typical example. A 20 mL scintillation vial equipped with a stir bar was filled with $^{OMe,iPr}(NNN^{cat})TaCl_2$ (0.11 g, 0.18 mmol, 1

dx.doi.org/10.1021/ic401496w | Inorg. Chem. 2013, 52, 11244−11255

equiv) and dissolved in 16 mL of THF. Next, finely ground [$NBnEt_3$][Cl] (0.04 g, 0.18 mmol, 1 equiv) was added to the vigorously stirred reaction mixture. After stirring for 12 h the solution was filtered. The solvent was removed from the filtrate under reduced pressure by coevaporation with a 6:1 (v/v) mixture of pentane/THF to afford the product as a fine red solid.

*[NEt_3Bn][^{OMe,iPr}(NNN^{cat})$TaCl_3$] (**5a**).* This material is prepared in 99% yield (0.15 g). Anal. Calcd for $C_{33}H_{48}N_4O_2Cl_3Ta$: C, 48.33; H, 5.90; N, 6.83. Found: C, 48.26; H, 6.02; N, 7.23. ^{1}H NMR (500 MHz, CD_3CN) δ/ppm: 7.50 (overlapping, 5H, NBn-H), 6.89 (d, $^3J_{HH}$ = 9 Hz, 2H, aryl-H), 6.10 (dd, $^3J_{HH}$ = 6 Hz, $^4J_{HH}$ = 2.5 Hz, 2H, aryl-H), 6.05 (d, $^3J_{HH}$ = 7.5 Hz, 2H, aryl-H), 5.32 (br, 2H, $CH(CH_3)_2$), 4.30 (s, 2H, NCH_2Ph), 3.70 (s, 6H, OCH_3), 3.12 (q, $^3J_{HH}$ = 7.0 Hz, 6H, NCH_2CH_3), 1.39 (d, $^3J_{HH}$ = 7 Hz, 12H, $CH(CH_3)_3$), 1.31 (t, $^3J_{HH}$ = 7.0 Hz, 9H, NCH_2CH_3). $^{13}C\{^1H\}$ NMR (118 Hz, CD_3CN) δ/ppm: 156.2 (ipso-C), 149.8 (ipso-C), 133.4 (ipso-C), 131.6 (ipso-C), 130.2 (aryl-C), 129.9 (aryl-C), 128.1 (aryl-C), 114.1 (aryl-C), 105.3 (aryl-C), 99.6 (aryl-C), 61.2 (N−CH_2Ph), 56.0 (OCH_3), 53.4 (N−CH_2CH_3), 49.9 ($CH(CH_3)_2$), 18.7 ($CH(CH_3)_3$), 8.1 (N−CH_2CH_3). UV−vis (THF) λ_{max}/nm (ε/M^{-1} cm^{-1}): 315 (18 300).

*[NEt_3Bn][^{F,iPr}(NNN^{cat})$TaCl_3$] (**5b**).* This material is prepared in 99% yield (0.11 g). Anal. Calcd for $C_{31}H_{42}N_3F_2Cl_3Ta$: C, 46.78; H, 5.32; N, 7.04. Found: C, 46.40; H, 5.32; N, 7.00. ^{1}H NMR (500 MHz, CD_3CN) δ/ppm: 7.50 (overlapping, 5H, NBn-H), 6.93 (dd, $^3J_{HH}$ = 6 Hz, $^4J_{HH}$ = 3 Hz, 2H, aryl-H), 6.55 (td, $^3J_{HF}$ = 9 Hz, $^4J_{HH}$ = 2.5 Hz, 2H, Ph-H), 630−6.21 (overlapping, 4H, aryl-H), 5.33 (sept, $^3J_{HH}$ = 6 Hz, 2H $CH(CH_3)_2$), 4.31 (s, 2H, NCH_2Ph), 3.12 (q, $^3J_{HH}$ = 7 Hz, 6H, NCH_2CH_3), 1.39 (d, $^3J_{HH}$ = 6.5 Hz, 12H, $CH(CH_3)_3$), 1.31 (t, $^3J_{HH}$ = 7 Hz, 9H, NCH_2CH_3). $^{13}C\{^1H\}$ NMR (118 Hz, CD_3CN) δ/ppm: 149.6 (ipso-C), 139.4 (ipso-C), 133.4 (ipso-C), 131.6 (ipso-C), 130.2 (aryl-C), 128.1 (aryl-C), 113.7 (d, J = 40 Hz, aryl-C), 105.6 (d, J = 90 Hz, aryl-C), 104.3 (d, J = 90 Hz, aryl-C), 99.8 (d, J = 103 Hz, aryl-C), 61.1 (NCH_2Ph), 53.4 (NCH_2CH_3), 50.4 ($CH(CH_3)_2$), 18.3 ($CH(CH_3)_3$), 8.1 (NCH_2CH_3). $^{19}F\{^1H\}$ NMR δ/ppm: −125.1. UV−vis (THF) λ_{max}/nm (ε/M^{-1} cm^{-1}): 310 (16 700).

*[NEt_3Bn][^{H,iPr}(NNN^{cat})$TaCl_3$] (**5c**).* This material was prepared in 99% yield (0.11 g). Anal. Calcd for $C_{31}H_{44}N_4Cl_3Ta$: C, 48.99; H, 5.84; N, 7.37. Found: C, 48.80; H, 5.97; N, 7.29. ^{1}H NMR (500 MHz, CD_3CN) δ/ppm: 7.50 (overlapping, 5H, NBn-H), 7.11 (d, $^3J_{HH}$ = 9 Hz, 1H, aryl-H), 6.55 (m, 4H, aryl-H), 6.46 (d, $^3J_{HH}$ = 9 Hz, 2H, aryl-H), 5.42 (sept, $^3J_{HH}$ = 8 Hz, 2H, $CH(CH_3)_2$), 4.30 (s, 2H, NCH_2Ph), 3.12 (q, $^3J_{HH}$ = 9 Hz, 6H, NCH_2CH_3), 1.41 (d, $^3J_{HH}$ = 8.5 Hz, 12H, $CH(CH_3)_3$), 1.33 (t, $^3J_{HH}$ = 9 Hz, 9H, NCH_2CH_3). $^{13}C\{^1H\}$ NMR (118 Hz, CD_3CN) δ/ppm: 149.0 (ipso-C), 143.4 (ipso-C), 133.5 (ipso-C), 131.6 (ipso-C), 130.3 (aryl-C), 128.1 (aryl-C), 122.1 (aryl-C), 120.7 (aryl-C), 115.0 (aryl-C), 112.9 (aryl-C), 61.2(NCH_2Ph), 53.5 (NCH_2CH_3), 50.0 ($CH(CH_3)_2$), 18.7 ($CH(CH_3)_3$), 8.2 (NCH_2CH_3). UV−vis (THF) λ_{max}/nm (ε/M^{-1} cm^{-1}): 310 (18 500).

*[NEt_3Bn][^{Me,iPr}(NNN^{cat})$TaCl_3$] (**5d**).* This material was prepared in 99% yield (0.12 g). Anal. Calcd for $C_{33}H_{48}N_4Cl_3Ta$: C, 50.29; H, 6.14; N, 7.11. Found: C, 49.90; H, 6.12; N, 6.92. ^{1}H NMR (500 MHz, CD_3CN) δ/ppm: 7.50 (overlapping, 5H, NBn-H), 6.94 (d, $^3J_{HH}$ = 8 Hz, 2H, aryl-H), 6.36 (d, $^3J_{HH}$ = 8 Hz, 2H, aryl-H), 6.30 (s, 2H, aryl-H), 5.38 (br, 2H $CH(CH_3)_2$), 4.29 (s, 2H, NCH_2Ph), 3.11 (q, $^3J_{HH}$ = 7 Hz, 6H, NCH_2CH_3), 2.32 (s, 6H, aryl-CH_3), 1.40 (d, $^3J_{HH}$ = 7 Hz, 12H, $CH(CH_3)_3$), 1.31 (t, $^3J_{HH}$ = 7.0 Hz, 9H, NCH_2CH_3). $^{13}C\{^1H\}$ NMR (118 Hz, CD_3CN) δ/ppm: 149.0 (ipso-C), 141.2 (ipso-C), 133.4 (ipso-C), 131.6 (ipso-C), 131.4 (aryl-C), 130.2 (aryl-C), 128.1 (aryl-C), 121.1 (aryl-C), 114.4 (aryl-C), 113.4 (aryl-C), 61.0 (NCH_2Ph), 53.4 (NCH_2CH_3), 49.7 ($CH(CH_3)_2$), 20.8 (aryl-CH_3), 18.6 ($CH(CH_3)_3$), 8.1 (NCH_2CH_3). UV−vis (THF) λ_{max}/nm (ε/M^{-1} cm^{-1}): 313 (14600).

*[NEt_3Bn][^{tBu,iPr}(NNN^{cat})$TaCl_3$] (**5e**).* This material was prepared in 99% yield (0.09 g). Anal. Calcd for $C_{39}H_{60}N_4Cl_3Ta$: C, 53.70; H, 6.93; N, 6.42. Found: C, 53.50; H, 6.90; N, 6.40. ^{1}H NMR (500 MHz, CD_3CN) δ/ppm: 7.50 (overlapping, 5H, NBn-H), 7.00 (d, $^3J_{HH}$ = 8.5 Hz, 2H, aryl-H), 6.60 (dd, $^3J_{HH}$ = 6.5 Hz, $^4J_{HH}$ = 2 Hz, 2H, aryl-H), 6.46 (d, $^4J_{HH}$ = 2 Hz, 2H, aryl-H), 5.42 (sept, $^3J_{HH}$ = 6.5 Hz, 2H $CH(CH_3)_2$), 4.33 (s, 2H, NCH_2Ph), 3.12 (q, $^3J_{HH}$ = 7.5 Hz, 6H, NCH_2CH_3), 1.42 (d, $^3J_{HH}$ = 6.5 Hz, 12H, $CH(CH_3)_3$), 1.31 (t, $^3J_{HH}$ = 7.5 Hz, 9H, NCH_2CH_3), 1.27 (s, 18H, aryl-^{t}Bu). $^{13}C\{^1H\}$ NMR (118 Hz, CD_3CN) δ/ppm: 148.8 (ipso-C), 144.8 (ipso-C), 141.4 (ipso-C), 133.4 (ipso-C), 131.6 (ipso-C), 130.3 (aryl-C), 128.2 (aryl-C), 117.6 (aryl-C), 114.2 (aryl-C), 110.0 (aryl-C), 61.1 (NCH_2Ph), 53.5 (NCH_2CH_3), 49.6 ($CH(CH_3)_2$), 34.4 ($C(CH_3)_3$), 32.0 ($C(CH_3)_3$), 18.8 ($CH(CH_3)_3$), 8.2 (NCH_2CH_3). UV−vis (THF) λ_{max}/nm (ε/M^{-1} cm^{-1}): 313 (17 400).

*[NEt_3Bn][^{OMe,DMP}(NNN^{cat})$TaCl_3$] (**5f**).* This material was prepared in 92% yield (0.15 g). Anal. Calcd for $C_{43}H_{52}N_4O_2Cl_3Ta(C_4H_8O)_{1.5}$: C, 55.92; H, 6.13; N, 5.32. Found: C, 56.27; H, 5.87; N, 5.60. ^{1}H NMR (500 MHz, CD_3CN) δ/ppm: 7.50 (overlapping, 5H, NCH_2Ph-H), 6.96 (d, $^3J_{HH}$ = 9 Hz, 2H, aryl-H), 6.90 (s, 4H, o-Ph-H), 6.87 (s, 2H, p-Ph-H), 6.14 (dd, $^3J_{HH}$ = 9 Hz, $^4J_{HH}$ = 3 Hz, 2H, aryl-H), 5.14 (d, $^4J_{HH}$ = 3 Hz, 2H, aryl-H), 4.30 (s, 2H, NCH_2Ph), 3.56 (s, 6H, O−CH_3), 3.11 (q, $^3J_{HH}$ = 8 Hz, 6H, NCH_2CH_3), 2.25 (s, 12H, aryl-CH_3), 1.32 (t, $^3J_{HH}$ = 8 Hz, 9H, NCH_2CH_3). $^{13}C\{^1H\}$ NMR (118 Hz, CD_3CN) δ/ppm: 157.2 (ipso-C), 154.3 (ipso-C), 145.9 (ipso-C), 139.4 (ipso-C), 134.9 (ipso-C), 133.4 (aryl-C), 131.6 (aryl-C), 130.2 (aryl-C), 129.2 (aryl-C), 128.1 (ipso-C), 126.8 (aryl-C), 114.6 (aryl-C), 106.6 (aryl-C), 98.5 (aryl-C), 61.0 (NCH_2Ph), 55.8 (aryl-OCH_3), 53.4 (NCH_2CH_3), 21.3 (aryl-CH_3), 8.2 (NCH_2CH_3).

General Preparation of ^{X,R}(NNN^{sq})$TaCl_3$. The new compounds were all prepared by a common procedure which is outlined for a typical example. Method A follows: A 20 mL scintillation vial equipped with a stir bar was filled with solid ^{H,iPr}(NNN^{cat})$TaCl_2$ (0.08 g, 0.15 mmol, 1 equiv) that was then dissolved in 10 mL of toluene. As the solution stirred, *N*-chlorosuccinimide (0.02 g, 0.16 mmol, 1.05 equiv) was added as a solid. After stirring for 12 h the solvent volume was reduced in vacuo (3 mL), and the brown solution was cooled (−35°) to induce precipitation of ^{H,iPr}(NNN^{sq})$TaCl_3$. The product was collected by filtration and dried under vacuum. Method B follows: A 20 mL scintillation vial equipped with a stir bar was filled with solid ^{Me,iPr}(NNN^{cat})$TaCl_2$ (0.07 g, 0.13 mmol, 1 equiv) that was then dissolved in THF (5 mL). The resulting red solution was chilled to −35 °C and then treated with a cold solution of $PhICl_2$ (0.02 g, 0.07 mmol, 0.5 equiv) in diethyl ether (10 mL). The reaction mixture was stored overnight at −35 °C. Complex ^{Me,iPr}(NNN^{sq})$TaCl_3$ precipitated as a dark green solid that was collected by filtration and dried under vacuum.

*^{OMe,iPr}(NNN^{sq})$TaCl_3$ (**6a**).* UV−vis (toluene) λ_{max}/nm (ε/M^{-1} cm^{-1}): 333 (27 000), 588 (4100), 1118 (3800). EPR (toluene, 298 K): g = 1.958; A_{iso} = 33 G.

*^{F,iPr}(NNN^{sq})$TaCl_3$ (**6b**).* This material is produced in a yield of 62% (0.07 g). Anal. Calcd for $C_{18}H_{22}N_3Cl_3Ta$: C, 35.81; H, 3.34; N, 6.96. Found: C, 36.38; H, 3.53; N, 6.64. UV−vis (toluene) λ_{max}/nm (ε/M^{-1} cm^{-1}): 326 (19 200), 553 (1900), 1151 (1900). EPR (toluene, 298 K): g = 1.964; A_{iso} = 30 G.

*^{H,iPr}(NNN^{sq})$TaCl_3$ (**6c**).* This material is produced in a yield of 53% (0.05 g). Anal. Calcd for $C_{18}H_{20}N_3Cl_3Ta$: C, 38.08; H, 3.91; N, 7.40. Found: C, 38.52 ; H, 4.26; N, 7.05. UV−vis (toluene) λ_{max}/nm (ε/M^{-1} cm^{-1}): 326 (23 700), 567 (1700), 1265 (2200). EPR (toluene, 298 K): g = 1.964 ; A_{iso} = 30 G.

*^{Me,iPr}(NNN^{sq})$TaCl_3$ (**6d**).* This material is produced in a yield of 43% (0.03 g). Anal. Calcd for $C_{20}H_{26}N_3Cl_3Ta$: C, 40.32; H, 4.40; N, 7.05. Found: C, 40.79; H, 4.80; N, 6.65. UV−vis (toluene) λ_{max}/nm (ε/M^{-1} cm^{-1}): 328 (25 300), 580 (2400), 1228 (2800). EPR (toluene, 298 K): g = 1.962; A_{iso} = 31 G.

*^{tBu,iPr}(NNN^{sq})$TaCl_3$ (**6e**).* This material is produced in a yield of 40% (0.04 g). Anal. Calcd for $C_{26}H_{38}N_3Cl_3Ta$: C, 45.93; H, 5.63; N, 6.18. Found: C, 46.19; H, 5.82; N, 6.49. UV−vis (toluene) λ_{max}/nm (ε/M^{-1} cm^{-1}): 330 (25 000), 576 (2100), 1237 (2100). EPR (toluene, 298 K): g = 1.962; A_{iso} = 31 G.

*^{OMe,DMP}(NNN^{sq})$TaCl_3$ (**6f**).* This material is produced in a yield of 53% (0.08 g). Anal. Calcd for $C_{26}H_{38}N_3Cl_3Ta(C_7H_8)_{0.25}$: C, 49.21; H, 4.16; N, 5.42. Found: C, 49.50; H, 4.35; N, 5.38. UV−vis (toluene) λ_{max}/nm (ε/M^{-1} cm^{-1}): 335 (29 000), 586 (4100), 1035 (4500). EPR (toluene, 298 K): g = 1.960; A_{iso} = 29 G.

General Procedure for the Preparation of ^{X,R}(NNN^{q})-$TaCl_2$(NPh-p-R′) (R′ = ^{t}Bu, CF_3, CH_3). The new compounds were all prepared by a common procedure, which is outlined for a typical

dx.doi.org/10.1021/ic401496w | Inorg. Chem. 2013, 52, 11244−11255

example. A 20 mL scintillation vial was charged with a toluene solution of ^{F,iPr}(NNN^{cat})TaCl$_2$ (0.05 g, 0.08 mmol, 1 equiv). ^{t}Bu-p-PhN$_3$ (0.02 g, 0.10 mmol, 1.2 equiv) was added dropwise resulting in a color change from dark red to brownish green. The solution was stirred overnight after which time the volatiles were removed and the resulting tacky solid was coevaporated and washed with pentane to give a greenish solid. X-ray quality crystals of **7a** and **7b** were obtained from chilled (−35 °C), saturated toluene solutions.

*^{F,iPr}(NNN^q)TaCl$_2$(NPh-p-^{t}Bu) (**7b**).* This material was prepared in 92% yield (0.06 g). ^{1}H NMR (400 MHz; CDCl$_3$) δ/ppm: 7.98 (dd, 2H, $^3J_{HH}$ = 9.0 Hz, J_{HF} = 6.0 Hz, aryl-H), 7.39 (d, 2H, $^3J_{HH}$ = 8.6 Hz, aryl-H), 7.23 (d, 2H, $^3J_{HH}$ = 8.6 Hz, aryl-H), 7.01−6.98 (overlapping, 4H total, aryl-H), 4.78 (m, 2H, CH(CH$_3$)$_2$), 1.71 (d, 12H, $^3J_{HH}$ = 6.5 Hz, CH(CH$_3$)$_2$), 1.34 (s, 9H, C(CH$_3$)$_3$). ^{13}C NMR (78 MHz; CDCl$_3$) δ/ppm: 166.9 (ipso-C), 164.6 (d, J_{CF} = 12 Hz, ipso-C), 153.3 (ipso-C), 147.3 (ipso-C), 139.1 (ipso-C), 127.5 (aryl-C), 126.0 (d, J_{CF} = 12 Hz, aryl-C), 124.9 (aryl-C), 118.7 (d, J_{CF} = 30 Hz, aryl-C), 102.1 (d, J_{CF} = 25 Hz, aryl-C), 56.7 (CH(CH$_3$)$_2$), 34.5 (C(CH$_3$)$_3$), 31.8 (C(CH$_3$)$_3$), 24.1 (CH(CH$_3$)$_2$). ^{19}F NMR (376.5 MHz; CDCl$_3$) δ/ppm: −96.9 (br). UV−vis (THF) λ_{max}/nm (ε/M^{-1} cm^{-1}): 299 (21 000), 369 (10 300), 533 (2500), 848 (8400).

*^{H,iPr}(NNN^q)TaCl$_2$(NPh-p-^{t}Bu) (**7c**).* Anal. Calcd for C$_{28}$H$_{35}$N$_4$Cl$_2$Ta: C, 49.50; H, 5.19; N, 8.25. Found: C, 49.12; H, 5.34; N, 8.11. 85% yield (0.04 g). ^{1}H NMR (400 MHz; CDCl$_3$) δ/ppm: 8.10 (d, 2H, $^3J_{HH}$ = 9.0 Hz, aryl-H), 7.51 (d, 2H, $^3J_{HH}$ = 9 Hz, aryl-H), 7.39 (overlapping, 4H total, aryl-H), 7.25 (d, 2H, $^3J_{HH}$ = 8 Hz, aryl-H), 7.17 (t, 2H, $^3J_{HH}$ = 7.5 Hz, aryl-H), 5.06 (br, 2H, CH(CH$_3$)$_2$), 1.75 (d, 12H, $^3J_{HH}$ = 6 Hz, CH(CH$_3$)$_2$), 1.35 (s, 9H, C(CH$_3$)$_3$). ^{13}C NMR (78 MHz; CDCl$_3$) δ/ppm: 163.0 (ipso-C), 153.6 (ipso-C), 146.8 (ipso-C), 142.5 (ipso-C), 135.2 (aryl-C), 127.7 (aryl-C), 127.4 (aryl-C), 124.9 (aryl-C), 124.5 (aryl-C),118.3 (aryl-C), 56.2 (CH(CH$_3$)$_2$), 34.4 (C(CH$_3$)$_3$), 31.8 (C(CH$_3$)$_3$), 24.4 (CH(CH$_3$)$_2$). UV−vis (THF) λ_{max}/nm (ε/M^{-1} cm^{-1}): 304 (25 000), 374 (10 500), 565 (1900), 884 (8500).

*^{Me,iPr}(NNN^q)TaCl$_2$(NPh-p-^{t}Bu) (**7d**).* Anal. Calcd for C$_{30}$H$_{39}$N$_4$Cl$_2$Ta: C, 50.93; H, 5.56; N, 7.92. Found: C, 50.52; H, 5.27; N, 7.74. Yield 83% (0.06 g). ^{1}H NMR (400 MHz; CDCl$_3$) δ/ppm: 7.98 (d, 2H, $^3J_{HH}$ = 9 Hz, aryl-H), 7.37 (d, 2H, $^3J_{HH}$ = 8 Hz, aryl-H), 7.25 (d, 2H, $^3J_{HH}$ = 8 Hz, aryl-H), 7.15 (br, 2H, aryl-H), 6.98 (d, 2H, $^3J_{HH}$ = 9 Hz, aryl-H), 5.02 (br, 2H, CH(CH$_3$)$_2$), 2.42 (s, 6H, aryl-CH$_3$), 1.74 (d, 12H, $^3J_{HH}$ = 6 Hz, CH(CH$_3$)$_2$), 1.35 (s, 9H, C(CH$_3$)$_3$). ^{13}C NMR (78 MHz; CDCl$_3$) δ/ppm: 163.0 (ipso-C), 153.8 (ipso-C), 147.0 (ipso-C), 146.6 (ipso-C), 140.8 (ipso-C), 130.0 (aryl-C), 127.4 (aryl-C), 124.8 (aryl-C), 123.9 (aryl-C), 116.8 (aryl-C), 55.6 (CH(CH$_3$)$_2$), 34.4 (C-(CH$_3$)$_3$), 31.8 (C(CH$_3$)$_3$), 24.4 (CH(CH$_3$)$_2$), 23.8 (aryl-CH$_3$). UV−vis (THF) λ_{max}/nm (ε/M^{-1} cm^{-1}): 306 (22 800), 379 (10 900), 553 (2200), 857 (9200).

*^{OMe,iPr}(NNN^q)TaCl$_2$(NPh-p-CF$_3$) (**8a**).* Anal. Calcd for C$_{27}$H$_{30}$N$_4$Cl$_2$F$_3$O$_2$Ta: C, 43.16; H, 4.02; N, 7.46. Found: C, 43.41; H, 3.88; N, 7.06. 81% yield (0.06 g). ^{1}H NMR (400 MHz; CDCl$_3$) δ/ppm: 7.95 (d, 2H, $^3J_{HH}$ = 9 Hz, aryl-H), 7.62 (d, 2H, $^3J_{HH}$ = 8 Hz, aryl-H), 7.39 (d, 2H, $^3J_{HH}$ = 8 Hz, aryl-H), 6.86 (dd, $^3J_{HH}$ = 9 Hz, $^4J_{HH}$ = 2 Hz, 2H total, aryl-H), 6.53 (d,$^4J_{HH}$ = 2 Hz, 2H, aryl-H) 4.86 (m, 2H, CH(CH$_3$)$_2$), 3.97 (s, 6H, OCH$_3$), 1.70 (d, 12H, $^3J_{HH}$ = 6 Hz, CH(CH$_3$)$_2$). ^{13}C NMR (78 MHz; CDCl$_3$) δ/ppm: 166.5 (ipso-C), 165.0 (ipso-C), 158.9 (ipso-C), 137.8 (aryl-C), 127.8 (aryl-C), 125.6 (aryl-C), 125.4 (aryl-C), 121.7 (aryl-C), 95.3 (aryl-C), 56.2 (OCH$_3$), 55.4 (CH(CH$_3$)$_2$), 24.2 (CH(CH$_3$)$_2$). ^{19}F NMR (376.5 MHz; CDCl$_3$) δ/ppm: −61.8 (br). UV−vis (THF) λ_{max}/nm (ε/M^{-1} cm^{-1}): 286 (25 300), 376 (12 300), 464 (9700), 528 (3800), 788 (11 000).

*^{F,iPr}(NNN^q)TaCl$_2$(NPh-p-CF$_3$) (**8b**).* This material was prepared in 84% yield (0.04 g). ^{1}H NMR (400 MHz; CDCl$_3$) δ/ppm: 8.04 (m, 2H, aryl-H), 7.65 (dd, 2H, $^3J_{HH}$ = 9 Hz, J_{HF} = 6 Hz, aryl-H), 7.38 (d, 2H, $^3J_{HH}$ = 8 Hz, aryl-H), 7.05−6.85 (overlapping, 4H total, Ph-H), 4.81 (m, 2H, CH(CH$_3$)$_2$), 1.68 (d, 12H, $^3J_{HH}$ = 6 Hz, CH(CH$_3$)$_2$). ^{19}F NMR (376.5 MHz; CDCl$_3$) δ/ppm: −61.9 (s, CF$_3$), −96.0 (s, aryl-F). ^{13}C NMR spectrum was not acquired due to the low solubility of the product. UV−vis (THF) λ_{max}/nm (ε/M^{-1} cm^{-1}): 302 (20 800), 370 (9200), 528 (2100), 847 (7100).

*^{OMe,DMP}(NNN^q)TaCl$_2$(NPh-p-CH$_3$) (**9f**).* Anal. Calcd for C$_{37}$H$_{37}$N$_4$Cl$_2$O$_2$Ta: C, 54.09; H, 4.54; N, 6.82. Found: C, 54.35; H, 4.51; N, 6.69. Yield 79% (0.14 g). ^{1}H NMR (400 MHz; CDCl$_3$) δ/ppm: 8.05 (d, $^3J_{HH}$ = 9 Hz, 2H, aryl-H), 7.13 (s, 4H, aryl-H), 6.97 (s, 2H, aryl-H), 6.80 (m, 2H, aryl-H), 6.73 (m, 2H, aryl-H), 6.05 (m, 2H, aryl-H), 5.50 (d, $^3J_{HH}$ = 9 Hz, 2H, aryl-H), 3.70 (s, 6H, O−CH$_3$), 2.35 (s, 12H, aryl-CH$_3$), 2.32 (s, 3H, aryl-CH$_3$). ^{13}C{^{1}H} NMR (128 MHz; CDCl$_3$; 298 K) δ/ppm: 166.5 (ipso-C), 166.3 (ipso-C), 152.7 (ipso-C), 149.3 (ipso-C), 139.2 (ipso-C), 137.3 (ipso-C), 132.8 (ipso-C), 128.2 (aryl-C), 127.1 (aryl-C), 126.6 (aryl-C), 125.4 (aryl-C), 122.6 (aryl-C), 121.9 (aryl-C), 97.6 (aryl-C), 56.1 (aryl-OCH$_3$), 21.4 (aryl-CH$_3$), 20.7 (aryl-CH$_3$). UV−vis (toluene) λ_{max}/nm (ε/M^{-1} cm^{-1}): 310 (29 700), 364 (19 200), 467 (12 700), 566 (5100), 773 (16 600). UV−vis (THF) λ_{max}/nm (ε/M^{-1} cm^{-1}): 309 (26 700), 364 (17 200), 466 (11 400), 566 (4600), 774 (15 000).

RESULTS AND DISCUSSION

Synthesis of ^{X,R}(NNN^{cat})H$_3$ Ligands. Previously, we described a three-step synthesis for the preparation of ^{OMe,iPr}(NNN^{cat})H$_3$ (**2a**, Scheme 1).[19] An Ullmann coupling of

Scheme 1

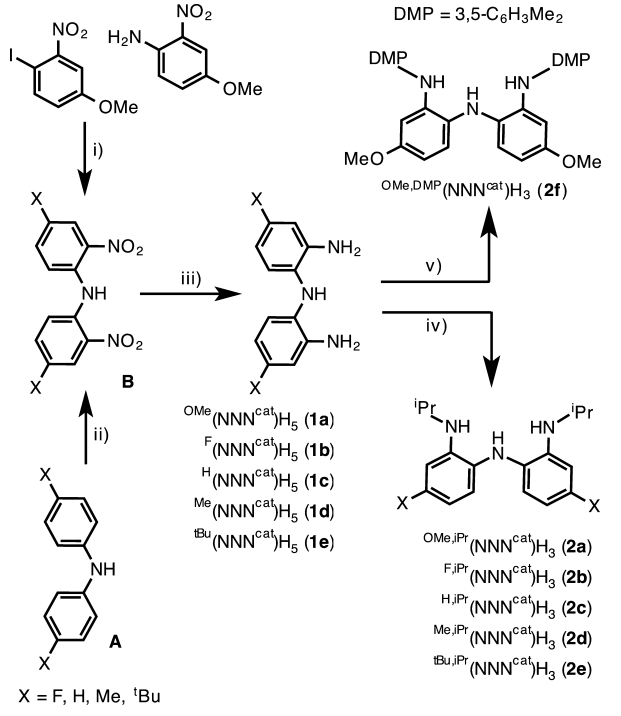

2-nitroanisidine and 3-iodo-4-nitroanisole with CuI gave the bis(2-nitro-4-methoxyphenyl)amine. Because similar starting materials are not commercially available for the other 4,4′-substituted ligand derivatives, a different approach was used to synthesize the ligand backbone of the general formula ^{X,iPr}(NNN^{cat})H$_3$ (X = F, **2b**; H, **2c**; Me, **2d**; tBu, **2e**). In each case, the appropriate diarylamine (A, Scheme 1) was reacted with isoamyl nitrite to effect selective nitration ortho to the central nitrogen atom and form the corresponding bis(2-nitro-4-X-phenyl)amine derivative (B, Scheme 1). The dinitro species were reduced with zinc metal and ammonium chloride to give the triammine derivatives **1a**−**e**. Reductive amination of

dx.doi.org/10.1021/ic401496w | Inorg. Chem. 2013, 52, 11244−11255

1a–e using acetone and sodium cyanoborohydride produced the isopropyl-substituted ligand precursors **2a–e** in 71–96% yield (Scheme 1). In order to test a different steric group on the (NNN) ligand platform, the related ligand $^{OMe,DMP}(NNN^{cat})H_3$ (DMP = 3,5-dimethylphenyl; **2f**) was prepared from **1a** and 3,5-dimethylbromobenzene via palladium-catalyzed cross-coupling. With 8 mol % loading of $Pd_2(dba)_3$, **2f** was obtained in multigram quantities and in 60–70% yields.[32]

Synthesis of $^{X,R}(NNN^{cat})^{3-}$ Complexes of Tantalum. Metalation of ligands **2b–f** proceed smoothly using trimethyltantalum dichloride as originally reported for **2a** (Scheme 2).[19]

Scheme 2

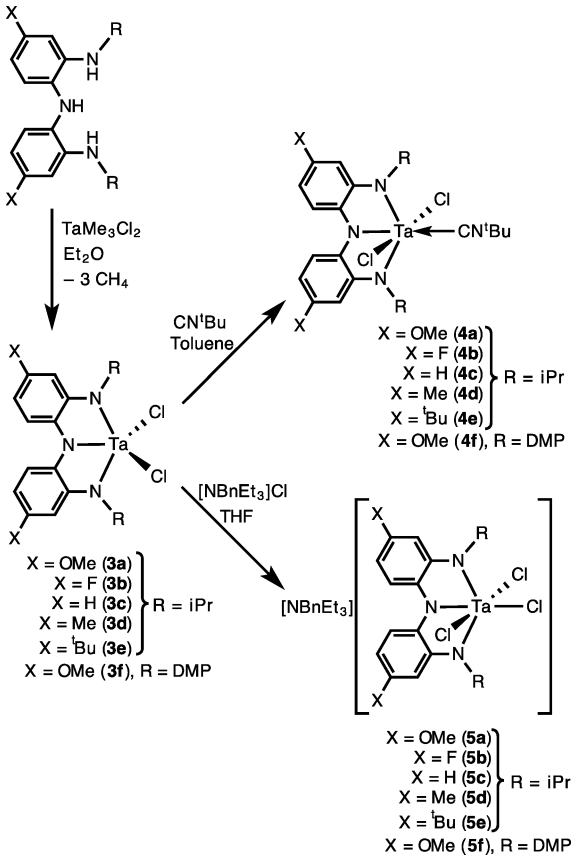

Treatment of the ligand precursors **2a–f** with cold diethyl ether solutions of $TaCl_2Me_3$ afforded the corresponding dichlorotantalum complexes $^{X,iPr}(NNN^{cat})TaCl_2$ (X = OMe, **3a**; F, **3b**; H, **3c**; Me, **3d**; ^{t}Bu, **3e**) and $^{OMe,DMP}(NNN^{cat})TaCl_2(OEt_2)$ (**3f**·Et_2O) upon loss of 3 equiv of methane. Depending on reaction conditions, the complexes can be isolated as the diethyl ether adducts, with derivative **3f** showing the greatest affinity for weakly coordinating solvents.

NMR spectroscopic data for **3a–e** are consistent with diamagnetic C_{2v}-symmetric tantalum(V) complexes. The ^{1}H and ^{13}C NMR spectra showed single resonances attributed to the methyl and methine moieties of the isopropyl groups; in addition, only one set of signals assigned to the backbone aryl resonances was observed.[19,33] The ^{1}H NMR spectrum of **3f**·Et_2O shows significant broadening of the resonances for the ligand backbone and for the coordinated ether molecule, suggesting an equilibrium between the six-coordinate ether adduct and a five-coordinate species analogous to that observed for **3a–e**.

Structural data for **3b–e** obtained by single-crystal X-ray diffraction revealed five-coordinate complexes in the solid state, consistent with the previously reported solid-state molecular structure for **3a**.[19] Figure 1a depicts an ORTEP of **3d** as a

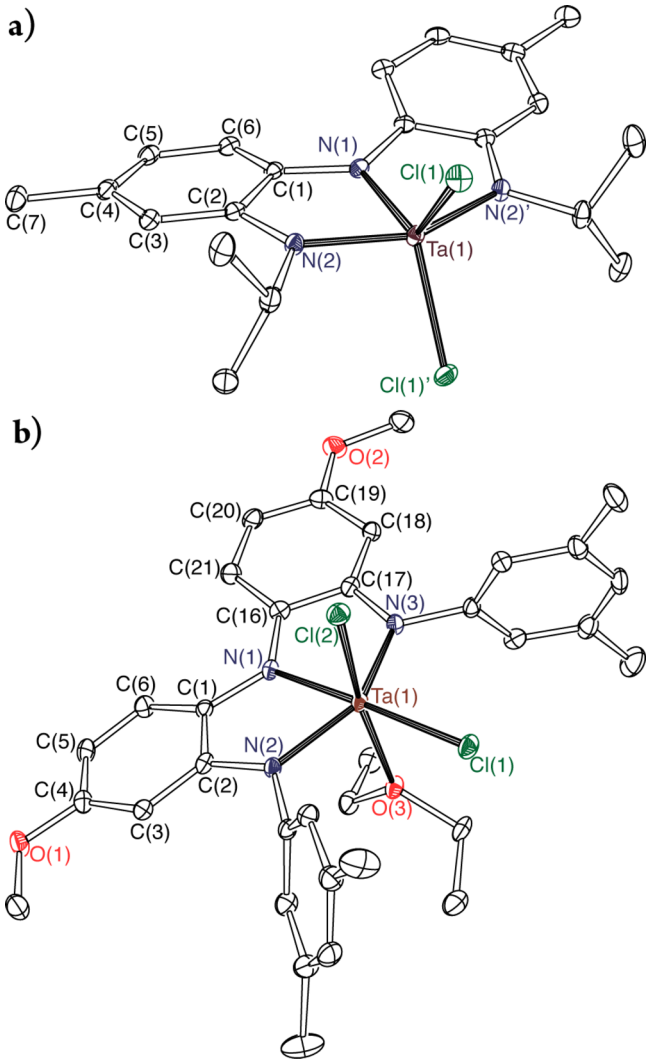

Figure 1. ORTEP diagrams showing thermal ellipsoids drawn at 50% probability for (a) $^{Me,iPr}(NNN^{cat})TaCl_2$ (**3d**) and (b) $^{OMe,DMP}(NNN^{cat})TaCl_2(OEt_2)$ (**3f**·Et_2O). Hydrogen atoms and cocrystallized solvent molecules have been omitted for clarity.

typical example of the structure type. Selected metrical parameters for **3a** (X = OMe), **3b** (X = F), and **3d** (X = Me) are listed in Table 1 (ORTEP diagrams and crystallographic data for **3b–f** are available as Supporting Information). Tantalum derivatives **3a–e** exhibit trigonal bipyramidal geometry around the tantalum center with the $(NNN^{cat})^{3-}$ ligand coordinated in a meridional fashion. The chloride ligands share the equatorial plane with the central nitrogen atom of the $(NNN^{cat})^{3-}$ ligand. The metal–ligand bond lengths for **3a–e** are within the expected ranges for tantalum(V) complexes, with minimal deviations in bond lengths between individual derivatives;[34–36] for example, the Ta–Cl bond lengths only vary between approximately 2.31 and 2.33 Å in **3a–e**. The carbon–nitrogen and carbon–carbon distances within the (NNN) ligand backbone are consistent with the fully reduced, catecholate form of the ligand.

dx.doi.org/10.1021/ic401496w | Inorg. Chem. 2013, 52, 11244–11255

Table 1. Selected Bond Lengths (Å) and Angles (deg) for $^{X,iPr}(NNN^{cat})TaCl_2$ (X = OMe, 3a; X = F, 3b; X = Me, 3d)

	3a[a]	3b	3d
	Bond Distances/Å		
Ta(1)−Cl(1)	2.3348(7)	2.3351(5)	2.3267(6)
Ta(1)−Cl(2)		2.3276(5)	
Ta(1)−N(1)	2.082(3)	2.0805(15)	2.077(3)
Ta(1)−N(2)	1.963(2)	1.9620(16)	1.995(2)
N(1)−C(1)	1.423(3)	1.424(2)	1.406(3)
N(2)−C(2)	1.383(3)	1.387(2)	1.388(3)
C(1)−C(2)	1.414(4)	1.411(3)	1.423(3)
C(2)−C(3)	1.385(4)	1.392(3)	1.393(3)
C(3)−C(4)	1.391(4)	1.377(3)	1.391(3)
C(4)−C(5)	1.390(4)	1.371(3)	1.416(4)
C(5)−C(6)	1.401(4)	1.391(3)	1.393(4)
C(6)−C(1)	1.383(4)	1.391(3)	1.388(3)
		Bond Angles/deg	
Cl(1)−Ta(1)−Cl(2)	120.72(3)	117.90(2)	113.28(3)

[a]Data taken from ref 19.

In contrast to **3a−e**, derivative **3f** crystallized as the six-coordinate diethyl ether adduct **3f**·Et_2O. Figure 1b shows the molecular structure of **3f**·Et_2O, which is best described as a distorted octahedron containing a meridional (NNN) ligand and two cis chloride ligands (selected metrical parameters shown in Table 3). In general, the six-coordinate environment of **3f**·Et_2O results in longer metal−ligand bonds than observed in **3a−e**. The Ta−Cl bonds are 2.38 Å (trans to N) and 2.39 Å (trans to OEt_2); similarly, the Ta−N bond lengths in **3f**·Et_2O are elongated by 0.03 Å compared to **3a−e**. The C_s symmetry of **3f**·Et_2O in the solid state supports the hypothesis that the symmetric NMR spectra for **3f** derive from reversible dissociation of the coordinated ether molecule on the NMR time scale.

The dichlorotantalum complexes $^{X,R}(NNN^{cat})TaCl_2$ (**3a−f**) reacted cleanly with ^{t}BuNC to generate dark red, six-coordinate adducts of the general formula $^{X,R}(NNN^{cat})TaCl_2(CN^tBu)$ (**4a−f**) as shown in Scheme 2. The ^{1}H and ^{13}C NMR spectra of **4a−f** indicate static structures on the NMR time scale. For complexes **4a−e**, the NMR data are consistent with C_{2v}-symmetric structures, indicating the presence of trans chloride ligands with the isocyanide ligand bound trans to the central nitrogen of the (NNN) ligand. In contrast, the NMR data for **4f** indicates a C_s-symmetric complex, requiring that the isocyanide binds trans to a chloride ligand, consistent with the solid-state structure of **3f**·Et_2O. The solid-state IR spectra of **4a−f** confirmed the coordination of the isocyanide ligand to an electron-poor tantalum(V) center since the complexes displayed C≡N stretch frequencies of $\nu_{C\equiv N} \sim 2203$ cm^{-1}, which is higher in frequency than the free isonitrile molecule (2125 cm^{-1}).[19,37−39]

In order to generate tantalum complexes stable for electrochemical analysis, chloride adducts of **3a−f** were prepared. Red THF solutions of **3a−f** were treated with $[NBnEt_3][Cl]$ to afford $[^{X,R}(NNN^{cat})TaCl_3]^-$ (R = iPr, X = OMe [**5a**]$^-$; X = F [**5b**]$^-$; X = H [**5c**]$^-$; X = Me [**5d**]$^-$; X = ^{t}Bu [**5e**]$^-$ and R = DMP, X = OMe [**5f**]$^-$) as dark red, $[NBnEt_3]^+$ salts that were insoluble in aromatic solvents. The ^{1}H and ^{13}C NMR spectra of **5a−f** in CD_3CN displayed resonances consistent with C_{2v}-symmetric, pseudo-octahedral species, consistent with a meridional (NNN) ligand and three meridional chloride ligands.

The electrochemistry of anions [**5a−f**]$^-$ was probed by cyclic voltammetry. In MeCN solvent using $[nBu_4N][PF_6]$ as the electrolyte, [**5a−f**]$^-$ have two partially reversible ($i_{pa} \geq i_{pc}$) one-electron oxidations. Figure 2 shows the cyclic voltammograms

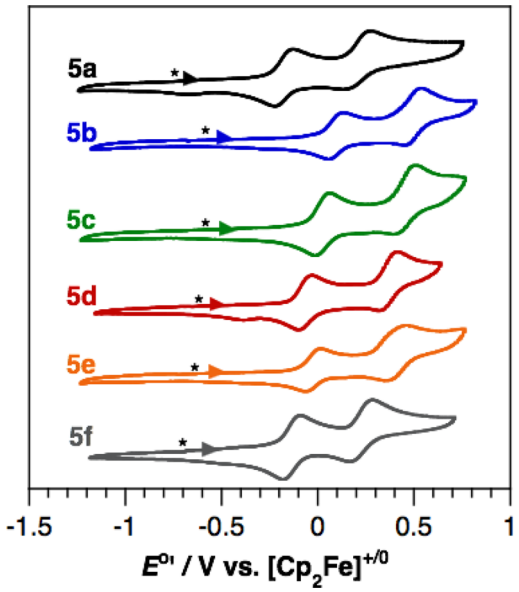

Figure 2. Cyclic voltammetry (MeCN, 0.1 M $[Bu_4N][PF_6]$ at 200 mV s^{-1}) of 1 mM solutions of (from top to bottom) $[^{F,iPr}(NNN^{cat})TaCl_3]^-$ (**5b**), $[^{H,iPr}(NNN^{cat})TaCl_3]^-$ (**5c**), $[^{tBu,iPr}(NNN^{cat})TaCl_3]^-$ (**5e**), $[^{Me,iPr}(NNN^{cat})TaCl_3]^-$ (**5d**), $[^{OMe,iPr}(NNN^{cat})TaCl_3]^-$ (**5a**), and $[^{OMe,DMP}(NNN^{cat})TaCl_3]^-$ (**5f**). The asterisk (*) denotes the potentials of the bulk tantalum complex. Potentials are referenced to $[Cp_2Fe]^{+/0}$.

Table 2. Electrochemical Properties of $[NBnEt_3][^{X,R}(NNN^{cat})TaCl_3]$ (5a−f)

			$E°2$ (V vs $[Cp_2Fe]^{+/0}$)	
X	R	compd	$[(NNN)TaCl_3]^{0/-}$	$[(NNN)TaCl_3]^{+/0}$
OMe	iPr	**5a**	−0.17	0.23
F	iPr	**5b**	0.10	0.50
H	iPr	**5c**	0.02	0.47
Me	iPr	**5d**	−0.07	0.36
tBu	iPr	**5e**	−0.02	0.42
OMe	DMP	**5f**	−0.13	0.23

for [**5a−f**]$^-$, and Table 2 summarizes the reduction potentials with respect to an internal $[Cp_2Fe]^{+/0}$ couple. Both redox potentials for [**5a−e**]$^-$ show a linear free energy relationship with the nature of the functional group in the ligand backbone. That is, derivative [**5b**]$^-$ with an electron-withdrawing fluoride substituent is oxidized at less positive potentials than derivative [**5a**]$^-$ with the electron-donating methoxy substituent. Comparison of [**5a**]$^-$ and [**5f**]$^-$ shows that the nitrogen substituent has a small effect on the ligand redox properties for the first oxidation and no measurable effect on the second oxidation.

One- and two-electron oxidized tantalum complexes are described here. Tantalum complexes of the one-electron oxidized $^{X,R}(NNN^{sq})^{2-}$ ligand were prepared by the addition of Cl$^\bullet$ to **3a−f**. The addition of 1 equiv of *N*-chlorosuccinimide or $^1/_2$ equiv of $PhICl_2$ to **3a−f** resulted in a rapid color change

dx.doi.org/10.1021/ic401496w | Inorg. Chem. 2013, 52, 11244−11255

from red to dark green signaling the formation of ^{X,R}(NNN^{sq})-$TaCl_3$ (R = iPr, X = OMe, **6a**; X = F, **6b**; X = H, **6c**; X = Me, **6d**; X = ^{t}Bu, **6e**; and R = DMP, X = OMe, **6f**), which were isolated as dark green microcrystalline solids in modest yields (Scheme 3).

Scheme 3

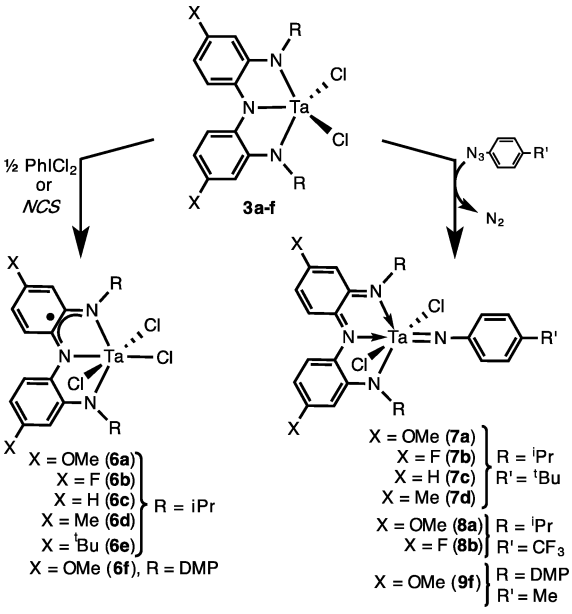

Complexes **6a**–**f** are paramagnetic, $S = {}^1/_2$ complexes with the unpaired electron localized primarily on the redox-active (NNN) ligand. The room-temperature EPR spectra of **6a**–**f** in toluene all display isotropic signals between g values of 1.958 and 1.964 with an eight-line pattern indicating hyperfine coupling to the $I = {}^7/_2$ tantalum center. The isotropic hyperfine coupling constants (a_{Ta}) for **6a**–**f** all fall in the range 29–33 G, which is significantly smaller than the coupling constants observed for well-define tantalum(IV) complexes.[19,40] A representative EPR spectrum for **6d** is shown in Figure 3, along with the corresponding simulated spectrum (see Supporting Information for the remaining EPR spectra). Also diagnostic for the semiquinonate oxidation state of the (NNN) ligand are the UV–vis–NIR spectra of **6a**–**f** that show ligand-based transitions in both the visible (λ_{max} = 550–590 nm) and near-IR (λ_{max} = 1120–1270 nm) portions of the spectrum (Figure 4).[6,19]

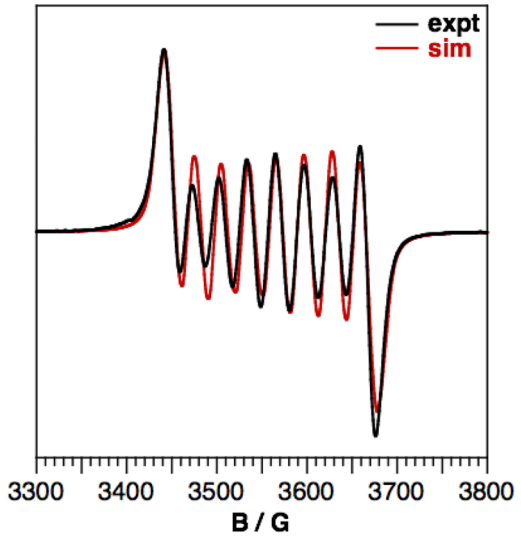

Figure 3. EPR spectrum of ^{Me,iPr}(NNN^{sq})$TaCl_3$ (**6d**) collected at 298 K in toluene (expt) and the corresponding simulated spectrum (sim).

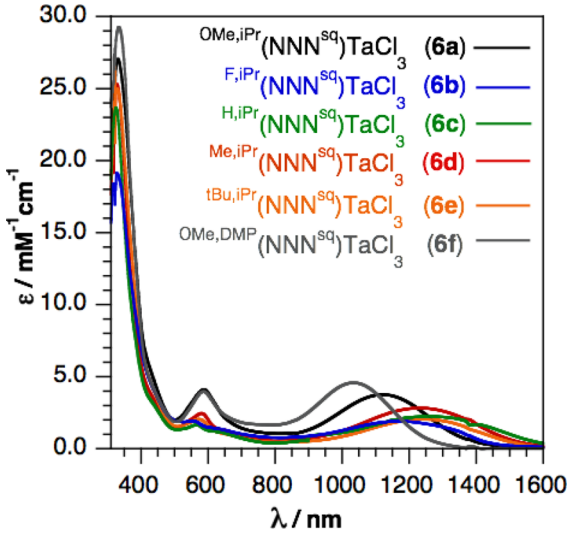

Figure 4. UV–vis–NIR spectra of ^{X,R}(NNN^{sq})$TaCl_3$ (**6a**–**f**) collected at 298 K in toluene: ^{OMe,iPr}(NNN^{sq})$TaCl_3$ (**6a**), ^{F,iPr}(NNN^{sq})$TaCl_3$ (**6b**), ^{H,iPr}(NNN^{sq})$TaCl_3$ (**6c**), ^{Me,iPr}(NNN^{sq})$TaCl_3$ (**6d**), ^{tBu,iPr}(NNN^{sq})$TaCl_3$ (**6e**), ^{OMe,DMP}(NNN^{sq})$TaCl_3$ (**6f**).

Single crystals of ^{OMe,DMP}(NNN^{sq})$TaCl_3$ (**6f**) were obtained and provided the first X-ray structural data for an (NNN) ligand in the semiquinonate oxidation state. An ORTEP of **6f** is depicted in Figure 5, and selected bond lengths and angles for

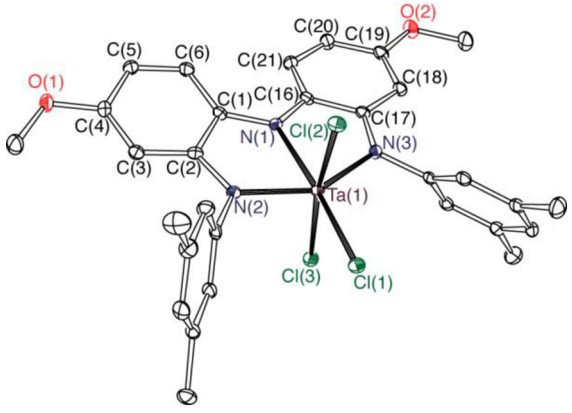

Figure 5. ORTEP diagram for ^{OMe,DMP}(NNN^{sq})$TaCl_3$ (**6f**). Thermal ellipsoids are drawn at 50% probability. Hydrogen atoms and cocrystallized solvent molecules have been omitted for clarity.

6f are displayed alongside those for the reduced congener ^{OMe,DMP}(NNN^{cat})$TaCl_2(OEt_2)$ (**3f**·Et_2O) in Table 3. As expected, **6f** displays a distorted octahedron geometry around the tantalum center, with a meridional arrangement of chloride ligands. As expected, the ligand N–C and C–C bond distances in the structure of **6f** fall between those observed for tantalum complexes of the fully reduced catecholate and fully oxidized quinonate ligands. For example, the semiquinonate oxidation state of the ligand in **6f** is evident from the N–C bond lengths,

dx.doi.org/10.1021/ic401496w | Inorg. Chem. 2013, 52, 11244–11255

Table 3. Selected Bond Lengths (Å) and Angles (deg) for $^{OMe,DMP}(NNN^{sq})TaCl_3$ (6f) and $^{OMe,DMP}(NNN^{cat})TaCl_2(OEt_2)$ (3f·Et$_2$O)

	6f	3f·Et$_2$O
	Bond Distances/Å	
Ta(1)−Cl(1)	2.3678(10)	2.3763(9)
Ta(1)−Cl(2)	2.3941(11)	2.3907(9)
Ta(1)−Z(3)	2.3846(10)[a]	2.222(2)[b]
Ta(1)−N(1)	2.215(3)	2.110(3)
Ta(1)−N(2)	2.008(3)	2.007(3)
Ta(1)−N(3)	2.021(3)	1.996(3)
N(1)−C(1)	1.387(5)	1.413(4)
N(2)−C(2)	1.377(5)	1.389(4)
N(1)−C(16)	1.367(5)	1.415(4)
N(3)−C(17)	1.375(5)	1.393(4)
C(1)−C(2)	1.419(5)	1.402(5)
C(16)−C(17)	1.418(5)	1.397(5)
O(1)−C(4)	1.363(5)	1.376(4)
O(2)−C(19)	1.354(5)	1.376(4)
	Bond Angles/deg	
Cl(2)−Ta(1)−Z(3)	171.83(3)[a]	169.09(3)[b]

[a]Z = Cl. [b]Z = OEt$_2$.

which are contracted by 0.03 Å relative to the N−C bonds of catecholate derivatives **3**, but elongated by 0.03 Å relative to the N−C bonds of quinonate derivatives **7** (vide infra).

Nitrene transfer to complexes **3a−f** was used to effect two-electron oxidation of the redox-active (NNN) ligand. As summarized in Scheme 3, the reaction of complexes **3a−f** with various aryl azides resulted in the liberation of N_2 and formation of the tantalum imido complexes $^{X,R}(NNN^q)TaCl_2(=N\text{-}p\text{-}C_6H_4R')$. Thus, **3b−d** were treated with $N_3(p\text{-}C_6H_4{}^tBu)$ giving $^{X,iPr}(NNN^q)TaCl_2(=N\text{-}p\text{-}C_6H_4{}^tBu)$ (X = F, **7b**; H, **7c**; Me, **7d**) in high yields. Tantalum imido complexes bearing an electron-withdrawing group on the arylimido ligand were synthesized by treating **3a** and **3b** with $N_3(p\text{-}C_6H_4CF_3)$ to generate $^{X,iPr}(NNN^q)TaCl_2(N\text{-}p\text{-}C_6H_4CF_3)$ (X = OMe, **8a**; F, **8b**). To determine if sterics would influence the nitrene transfer reaction, **3f**·Et$_2$O was treated with $N_3(p\text{-}C_6H_4CH_3)$ to give $^{OMe,R}(NNN^q)TaCl_2(N\text{-}p\text{-}C_6H_4CH_3)$ (**9f**). The compounds were isolated as microcrystalline brown to green solids that were sparingly soluble in aromatic solvents. NMR spectra in $CDCl_3$ of **7−9** are consistent with diamagnetic C_{2v}-symmetric tantalum(V) complexes. The symmetry of **9f** was assigned on the basis of the ^{1}H NMR spectra, which showed only one resonance corresponding to the ortho protons of the DMP substituent, indicating that the imido ligand is trans to the central nitrogen of the (NNN) scaffold, as observed in the other imido complexes.

Tantalum complexes **7−9** all have rich absorbance spectra with features throughout the UV−vis−NIR regions. Figure 6 shows the electronic absorption spectra of **7a**, **7b**, **8a**, **8b**, and **9f** to illustrate the impact that changes to the redox-active (NNN) ligand and to the terminal imido ligand have on the electronic properties of the complexes. Sharp transitions between 300 and 500 nm are complimented by a broad and intense absorption in the red portion of the spectrum.[6,19] The electronic substituent, X, on the (NNN) ligand has a measurable effect on the low-energy transition as can be seen by comparing **7a** to **7b** or **8a** to **8b** in Figure 6. The more electron-withdrawing flouride of **7b** and **8b** resulted in a 60 nm red shift of the band compared to the electron-donating methoxy substituent of **7a** and **8a**. On the other hand, comparing the spectrum of **7a** and **9f** suggests that the steric substituent, R, on the (NNN) ligand has a negligible impact on the energy of the absorption bands. Similarly, the imido substituent has no effect on the energy or intensity of the absorption features (compare **7a** to **8a** or **7b** to **8b**). Taken together, these results suggest that the frontier electronic structure of **7−9** is dominated by the diaryl backbone of the (NNN) ligand.

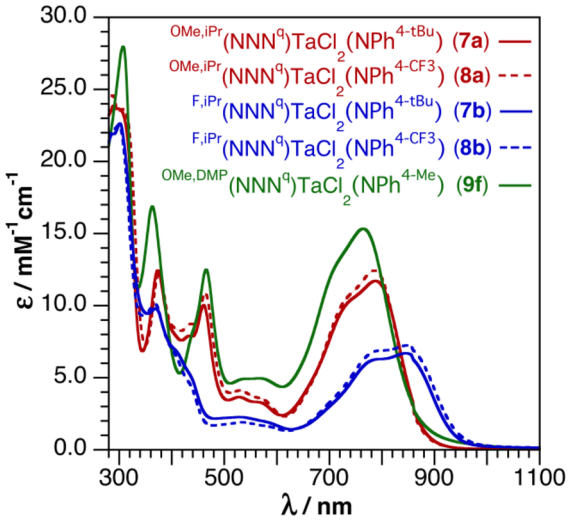

Figure 6. UV−vis−NIR spectra of $^{OMe,iPr}(NNN^q)TaCl_2(NPh^{4\text{-}tBu})$ (**7a**), $^{OMe,iPr}(NNN^q)TaCl_2(NPh^{4\text{-}CF3})$ (**8a**), $^{F,iPr}(NNN^q)TaCl_2(NPh^{4\text{-}tBu})$ (**7b**), $^{F,iPr}(NNN^q)TaCl_2(NPh^{4\text{-}CF3})$ (**8b**), and $^{OMe,DMP}(NNN^q)TaCl_2(NPh^{4\text{-}Me})$ (**9f**) collected at 298 K in THF.

Single crystals suitable for X-ray diffraction studies were obtained for $^{OMe,iPr}(NNN^q)TaCl_2(=N\text{-}p\text{-}C_6H_4{}^tBu)$ (**7a**) and for $^{Me,iPr}(NNN^q)TaCl_2(=N\text{-}p\text{-}C_6H_4{}^tBu)$ (**7d**). Figure 7 shows

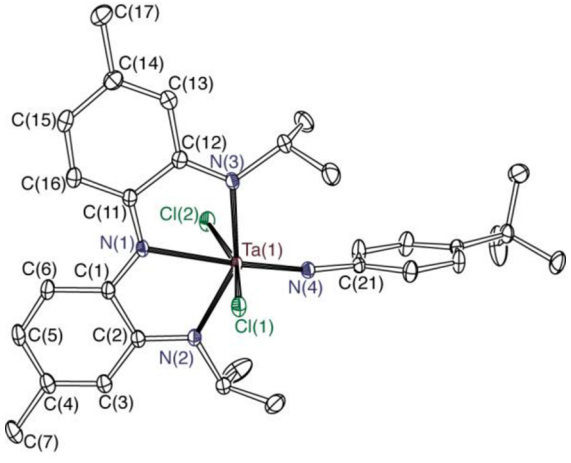

Figure 7. ORTEP diagram for $^{Me,iPr}(NNN^q)TaCl_2(=N\text{-}p\text{-}C_6H_4{}^tBu)$ (**7d**). Thermal ellipsoids are drawn at 50% probability. Hydrogen atoms and cocrystallized solvent molecules have been omitted for clarity.

an ORTEP diagram for **7d**, which is directly analogous to the structure for **7a**; Table 4 presents selected bond metrics for **7d** alongside those for **7a**. In short, the structures for **7a** and **7d** are indistinguishable with bond length differences of less than 0.01 Å.

dx.doi.org/10.1021/ic401496w | Inorg. Chem. 2013, 52, 11244−11255

Table 4. Selected Bond Lengths (Å) and Angles (deg) for $^{X,iPr}(NNN^{q})TaCl_2(=N\text{-}p\text{-}C_6H_4{}^{t}Bu)$ (X = OMe, 7a; X = Me, 7d)

	X = OMe (7a)	X = Me (7d)
Bond Distances/Å		
Ta(1)−N(4)	1.793(2)	1.790(2)
Ta(1)−Cl(1)	2.4393(8)	2.4345(7)
Ta(1)−Cl(2)	2.4248(8)	2.4355(7)
Ta(1)−N(1)	2.272(2)	2.281(2)
Ta(1)−N(2)	2.119(2)	2.128(2)
Ta(1)−N(3)	2.132(3)	2.125(2)
N(1)−C(1)	1.352(4)	1.353(3)
N(2)−C(2)	1.347(4)	1.348(3)
N(1)−C(11)	1.342(4)	1.341(3)
N(3)−C(12)	1.338(4)	1.345(3)
C(1)−C(2)	1.460(4)	1.460(4)
C(11)−C(12)	1.465(4)	1.461(4)
X−C(4)	1.357(4)	1.503(4)
X−C(14)	1.350(4)	1.503(4)
	Bond Angles/deg	
Ta(1)−N(4)−C(21)	171.4(2)	167.1(2)

CONCLUDING REMARKS

A family of tantalum complexes containing derivatives of the redox-active (NNN) ligand have been prepared and characterized by a battery of analytical techniques with the goal of benchmarking the impact of different electronic and steric substituents on the ligand. Five ligand derivatives with different electronic substituents incorporated into the ligand backbone were studied, including OMe, tBu, Me, H, and F. On the basis of electrochemical data, collected on $[^{X,iPr}(NNN^{cat})TaCl_3]^-$ derivatives **5a−e**, these groups rank from the most electron donating, OMe, to the least donating, F, affording a 270 mV range for the reduction potentials of the tantalum complexes. The electronically different (NNN) ligands also manifest differences in the UV−vis−NIR spectra of complexes containing the oxidized $^{X,R}(NNN^{sq})^{2-}$ or $^{X,R}(NNN^{q})^{-}$ ligands. In these cases, the lowest-energy absorption band is sensitive to the electronic group of the (NNN) ligand with electron-releasing methoxy groups pushing the absorption to higher energy and the electron-withdrawing fluoro groups pushing the absorption to lower energy. This effect was small, encompassing differences in λ_{max} of only 30 to 60 nm; moreover, the data suggests that these transitions are $\pi \rightarrow \pi^*$ transitions localized entirely on the backbone of the (NNN) ligand with little to no participation from the tantalum center or from the ancillary ligands.

Despite the readily measurable differences in redox potentials for the electronic derivatives of the (NNN) ligand platform, these substituents did not manifest significant changes to the structural or spectroscopic properties of the various tantalum complexes studied. Isonitrile stretching frequencies in **4a−e** were identical, suggesting that all $^{X,R}(NNN^{cat})^{3-}$ ligand derivatives act as similar electron donors to the tantalum(V) center. Similarly, EPR spectra of the $S = {}^1/_2$ complexes **6a−e** showed no difference in g or isotropic a_{Ta} values, indicating a similar degree of delocalization of the free electron between the $^{X,R}(NNN^{sq})^{2-}$ ligand and the tantalum center across the series of complexes. Finally, the structures of imido complexes **7a** and **7d** showed differences of less than 0.01 Å in the metal−ligand bond lengths (including the Ta=NR bond) suggesting that the different electronic substituents in $^{X,R}(NNN^{q})^{-}$ ligands have minimal impact on the coordination chemistry at the tantalum center. It can be concluded that the 270 mV potential range set forth by the electrochemistry of complexes **6a−e** does not change appreciably the nature of the metal−ligand interaction between the tantalum center and the (NNN) ligand: across five ligand derivatives, and in each ligand oxidation state, the redox-active frontier orbital of the tantalum complexes is localized primarily on the ligand. For other, less electropositive metals, this conclusion may not hold, as more extensive mixing[15] between metal d orbitals and ligand-based orbitals could lead to changes in the interactions between the metal center and the ancillary ligands.

A sixth ligand derivative, $^{OMe,DMP}(NNN^{cat})H_3$ (**2f**), containing the methoxy group in the backbone and 3,5-dimethylphenyl steric groups, was used to probe the impact of different sterics surrounding the metal center. Despite the fact that aryl groups can significantly modulate π-interactions in amido-type ligands, changing the steric substituent on the (NNN) ligand from isopropyl to 3,5-dimethylphenyl had little effect on the ligand redox potentials as evidenced by the nearly identical cyclic voltammograms for **5a** and **5f**, respectively. Similarly, comparisons of the UV−vis−NIR absorption spectra of **6a** and **6f** or **7a** and **9f**, revealed only minor shifts in the absorption bands resulting from inclusion of the DMP groups. The DMP groups did impact coordination geometry though, as evidenced in the NMR and structural data for **3f**·Et_2O and **4f**. In these complexes the data suggests that the DMP groups facilitate formation of a C_s symmetric structure with cis chloride ligands as opposed to the C_{2v} symmetric structure with trans chloride ligands that is observed for all isopropyl derivatives **3a−e** and **4a−e**. While it is not clear why the DMP-substituted (NNN) ligand affords a different coordination isomer for tantalum complexes **3f**·Et_2O and **4f**, it provides another synthetic strategy for controlling substrate binding in small molecule activation reactions.

ASSOCIATED CONTENT

Supporting Information

X-ray diffraction data (in CIF format) for **3b−f**, **6f**, **7a**, and **7d**. ORTEP diagrams of the molecular structures, and EPR, UV−vis−NIR and NMR spectra. This material is available free of charge via the Internet at http://pubs.acs.org.

AUTHOR INFORMATION

Corresponding Author

*E-mail: aheyduk@uci.edu.

Notes

The authors declare no competing financial interest.

ACKNOWLEDGMENTS

This work was supported by the NSF (CHE-1152543). The authors thank Dr. Joseph W. Ziller for assistance with analysis of X-ray diffraction data. A.F.H. is a Camille Dreyfus Teacher-Scholar.

REFERENCES

(1) Munhá, R. F.; Zarkesh, R. A.; Heyduk, A. F. *Dalton Trans.* **2013**, *43*, 3751−3766.

(2) Wong, J. L.; Hernandez Sanchez, R.; Glancy Logan, J.; Zarkesh, R. A.; Ziller, J. W.; Heyduk, A. F. *Chem. Sci.* **2013**, *4*, 1906−1910.

(3) Tondreau, A. M.; Stieber, S. C. E.; Milsmann, C.; Lobkovsky, E.; Weyhermueller, T.; Semproni, S.; Chirik, P. J. *Inorg. Chem.* **2013**, *52*, 635−646.

(4) Darmon, J. M.; Stieber, S. C. E.; Sylvester, K.; Fernandez, I.; Lobkovsky, E.; Semproni, S. P.; Bill, E.; Wieghardt, K.; DeBeer, S.; Chirik, P. J. *J. Am. Chem. Soc.* **2012**, *134*, 17125−17137.
(5) Marshall-Roth, T.; Liebscher, S. C.; Rickert, K.; Seewald, N. J.; Oliver, A. G.; Brown, S. N. *Chem. Commun.* **2012**, *48*, 7826−7828.
(6) Heyduk, A. F.; Zarkesh, R. A.; Nguyen, A. I. *Inorg. Chem.* **2011**, *50*, 9849−9863.
(7) Lippert, C. A.; Arnstein, S. A.; Sherrill, C. D.; Soper, J. D. *J. Am. Chem. Soc.* **2010**, *132*, 3879−3892.
(8) Chirik, P. J.; Wieghardt, K. W. *Science* **2010**, *327*, 794−795.
(9) Ringenberg, M. R.; Kokatam, S. L.; Heiden, Z. M.; Rauchfuss, T. B. *J. Am. Chem. Soc.* **2008**, *130*, 788−789.
(10) Stanciu, C.; Jones, M. E.; Fanwick, P. E.; Abu-Omar, M. M. *J. Am. Chem. Soc.* **2007**, *129*, 12400−12401.
(11) Bart, S. C.; Lobkovsky, E.; Bill, E.; Wieghardt, K.; Chirik, P. J. *Inorg. Chem.* **2007**, *46*, 7055−7063.
(12) Bart, S. C.; Chlopek, K.; Bill, E.; Bouwkamp, M. W.; Lobkovsky, E.; Neese, F.; Wieghardt, K.; Chirik, P. J. *J. Am. Chem. Soc.* **2006**, *128*, 13901−13912.
(13) Yin, C.-X.; Finke, R. G. *J. Am. Chem. Soc.* **2005**, *127*, 9003−9013.
(14) Weiner, H.; Finke, R. G. *J. Am. Chem. Soc.* **1999**, *121*, 9831−9842.
(15) Masui, H.; Lever, A. B. P.; Auburn, P. R. *Inorg. Chem.* **1991**, *30*, 2402−2410.
(16) Darmon, J. M.; Turner, Z. R.; Lobkovsky, E.; Chirik, P. J. *Organometallics* **2012**, *31*, 2275−2285.
(17) Zhu, D.; Budzelaar, P. H. M. *Organometallics* **2008**, *27*, 2699−2705.
(18) Hananouchi, S. P.; Zarkesh, R. A.; Ziller, J. W.; Heyduk, A. F. Unpublished results.
(19) Nguyen, A. I.; Blackmore, K. J.; Carter, S. M.; Zarkesh, R. A.; Heyduk, A. F. *J. Am. Chem. Soc.* **2009**, *131*, 3307−3316.
(20) Zarkesh, R. A.; Ziller, J. W.; Heyduk, A. F. *Angew. Chem., Int. Ed.* **2008**, *47*, 4715−4718.
(21) Lever, A. B. P. *Coord. Chem. Rev.* **2010**, *254*, 1397−1405.
(22) Zhao, H.; Tanjutco, C.; Thayumanavan, S. *Tetrahedron Lett.* **2001**, *42*, 4421−4424.
(23) Fan, L.; Yang, L.; Guo, C.; Foxman, B. M.; Ozerov, O. V. *Organometallics* **2004**, *23*, 4778−4787.
(24) Ren, P.; Vechorkin, O.; von Allmen, K.; Scopelliti, R.; Hu, X. *J. Am. Chem. Soc.* **2011**, *133*, 7084−7095.
(25) Schrock, R. R.; Sharp, P. R. *J. Am. Chem. Soc.* **1978**, *100*, 2389−2399.
(26) *SMART Software Users Guide, Version 5.1*; Bruker Analytical X-ray Systems, Inc.: Madison, WI, 1999.
(27) *SAINT Software Users Guide, Version 6.0*; Bruker Analytical X-ray Systems, Inc.: Madison, WI, 1999.
(28) Sheldrick, G. M. *SADABS, Version 2.10*; Bruker Analytical X-ray Systems, Inc.: Madison, WI, 2002.
(29) Sheldrick, G. M. *SHELXTL, Version 6.12*; Bruker Analytical X-ray Systems, Inc.: Madison, WI, 2001.
(30) *International Tables for X-ray Crystallography*; Kluwer Academic Publishers: Dordrecht, 1992; Vol. C.
(31) Farrugia, L. J. *J. Appl. Crystallogr.* **1997**, *30*, 565.
(32) Wolfe, J. P.; Wagaw, S.; Buchwald, S. L. *J. Am. Chem. Soc.* **1996**, *118*, 7215−7216 and references cited.
(33) Nguyen, A. I.; Zarkesh, R. A.; Lacy, D. C.; Thorson, M. K.; Heyduk, A. F. *Chem. Sci.* **2011**, *2*, 166−169.
(34) Spencer, L. P.; Beddie, C.; Hall, M. B.; Fryzuk, M. D. *J. Am. Chem. Soc.* **2006**, *128*, 12531−12543.
(35) Tanski, J. M.; Parkin, G. *Inorg. Chem.* **2003**, *42*, 264−266.
(36) Guzei, I. A.; Yap, G. P. A.; Winter, C. H. *Inorg. Chem.* **1997**, *36*, 1738−1739.
(37) Guo, Z. Y.; Swenson, D. C.; Guram, A. S.; Jordan, R. F. *Organometallics* **1994**, *13*, 766−773.
(38) Gomez, M.; Gomez-Sal, P.; Nicolas, M. P.; Royo, P. *J. Organomet. Chem.* **1995**, *491*, 121−125.
(39) Royo, P.; Sanchez-Nieves, J. *J. Organomet. Chem.* **2000**, *597*, 61−68.
(40) Noh, W.; Girolami, G. S. *Inorg. Chem.* **2008**, *47*, 535−542.